Ric-8 Proteins Are Molecular Chaperones That Direct Nascent G Protein α Subunit Membrane Association

Meital Gabay[1], **Mary E. Pinter**[1], **Forrest A. Wright**[1], **PuiYee Chan**[1], **Andrew J. Murphy**[2], **David M. Valenzuela**[2], **George D. Yancopoulos**[2], and **Gregory G. Tall**[1,*]

[1]Department of Pharmacology and Physiology, University of Rochester Medical Center, Rochester, NY 14642, USA

[2]Regeneron Pharmaceuticals Inc., Tarrytown, NY 10510, USA

Abstract

Ric-8A (resistance to inhibitors of cholinesterase 8A) and Ric-8B are guanine nucleotide exchange factors that enhance different heterotrimeric guanine nucleotide–binding protein (G protein) signaling pathways by unknown mechanisms. Because transgenic disruption of *Ric-8A* or *Ric-8B* in mice caused early embryonic lethality, we derived viable *Ric-8A–* or *Ric-8B*–deleted embryonic stem (ES) cell lines from blastocysts of these mice. We observed pleiotropic G protein signaling defects in *Ric-8A*$^{-/-}$ ES cells, which resulted from reduced steady-state amounts of $G\alpha_i$, $G\alpha_q$, and $G\alpha_{13}$ proteins to <5% of those of wild-type cells. The amounts of $G\alpha_s$ and total Gβ protein were partially reduced in *Ric-8A*$^{-/-}$ cells compared to those in wild-type cells, and only the amount of $G\alpha_s$ was reduced substantially in *Ric-8B*$^{-/-}$ cells. The abundances of mRNAs encoding the G protein α subunits were largely unchanged by loss of *Ric-8A* or *Ric-8B*. The plasma membrane residence of G proteins persisted in the absence of *Ric-8* but was markedly reduced compared to that in wild-type cells. Endogenous $G\alpha_i$ and $G\alpha_q$ were efficiently translated in *Ric-8A*$^{-/-}$ cells but integrated into endomembranes poorly; however, the reduced amounts of G protein α subunits that reached the membrane still bound to nascent Gβγ. Finally, $G\alpha_i$, $G\alpha_q$, and $G\beta_1$ proteins exhibited accelerated rates of degradation in *Ric-8A*$^{-/-}$ cells compared to those in wild-type cells. Together, these data suggest that Ric-8 proteins are molecular chaperones required for the initial association of nascent Gα subunits with cellular membranes.

INTRODUCTION

Resistance to inhibitors of cholinesterase 8A (Ric-8A) and Ric-8B are guanine nucleotide exchange factors (GEFs) for the α subunits of heterotrimeric guanine nucleotide–binding proteins (G proteins) (1, 2). Ric-8A stimulates the intrinsic nucleotide exchange rates of three of the four classes of G protein α subunits, $G\alpha_i$, $G\alpha_q$, and $G\alpha_{12/13}$, whereas Ric-8B is a

---

SUPPLEMENTARY MATERIALS

www.sciencesignaling.org/cgi/content/full/4/200/ra79/DC1

Fig. S1. Genomic PCR scheme to genotype *Ric-8A–* and *Ric-8B*–deleted mice and derived mES cell lines.

Fig. S2. Increased abundance of Gβγ does not rescue the defects in Gα protein abundance observed in *Ric-8*$^{-/-}$ cells.

Fig. S3. Nascent $G\alpha_i$ appears to be differentially modified in *Ric-8A*$^{-/-}$ and wild-type cells by means other than myristoylation.

Fig. S4. Forskolin-stimulated cAMP production is blunted in *Ric-8A*$^{-/-}$ and *Ric-8B*$^{-/-}$ cells compared to that in wild-type cells.

GEF for Gα$_s$. *RIC-8* was discovered during a genetic screen of *Caenorhabditis elegans* that was designed to uncover mutants with defective neurotransmitter release (3). Genetically, the single *C. elegans* Ric-8 protein was predicted to act upstream of, or in parallel with, Gα$_q$ and Gα$_s$ to regulate synaptic vesicle priming and to work with Gα$_o$ to control centrosome movements (4-6). The role of Ric-8 in regulation of mitotic spindle pole movements with complexes containing Gα$_{i/o}$ and GoLoco proteins has been dissected in detail and is conserved in worms, flies, and mammals (7-12). In mammalian cells, Ric-8A appears to potentiate Gα$_q$ signaling, and Ric-8B overexpression enhances activation of adenylyl cyclase (AC) by G$_s$ and G$_{olf}$ (13-15). This latter finding resulted in a technical advance, namely, that Ric-8B enabled efficient odorant coupling to G$_{olf}$ in human embryonic kidney (HEK) 293 cells reconstituted with odorant receptors (16, 17).

The positive roles that Ric-8 proteins have on divergent G protein signaling pathways are consistent with the capacities of Ric-8A and Ric-8B to collectively act as GEFs for all classes of G protein α subunits; however, there has been no demonstration of the GEF activities of Ric-8 proteins in cells, and it is unclear whether they directly activate G proteins to evoke effector enzyme signaling outputs. An alternative hypothesis for the regulation of G protein function by Ric-8 proteins was originally proposed from work with *Drosophila* Ric-8. Mutants of *Drosophila* Ric-8 or Ric-8–specific RNA interference (RNAi) result in defective asymmetric cell division and, consequently, the unorganized gastrulation of embryos and differentiation of neuroblasts (18-20). The abundances of Gα$_{i/o}$ and Gβ proteins are also reduced in these mutants, and these G proteins are mislocalized to undescribed cytosolic puncta. Similarly, a reduction in the amount of the Gα$_i$ homolog Gpa16 in so-called cortical crescents (plasma membrane) is observed in mitotic *ric-8* reduction-of-function mutant *C. elegans* embryos (21). Ric-8B enhances the amounts of Gα$_{olf}$ and Gα$_s$ in cultured mammalian cells (13, 22). The abundance of recombinant G protein α subunit in *Sf9* insect cells was increased greatly by co-infection with recombinant Ric-8A– or Ric-8B–expressing baculoviruses and provided an enhanced method for the purification of all classes of G protein α subunits (23). Together, these results suggest that a function of Ric-8 proteins is to promote G protein biosynthesis or to stabilize mature G proteins.

G protein biosynthesis is a complex process that begins with the translation of Gα, Gβ, and Gγ subunits on free ribosomes. The cytosolic chaperonin–containing t-complex polypeptide 1 (CCT) mediates the folding of Gα$_t$ (transducin) and Gβ (24, 25). The co-chaperone protein phosducin-like protein-1 (PhLP-1) acts with CCT to fold nascent Gβ subunits and assemble Gβγ dimers. Gβ is released from the CCT in a complex with PhLP-1. Dopamine receptor–interacting protein 78 (DRIP78)–promoted folding of nascent Gγ precedes the formation of a PhLP-1–GβGγ ternary complex that translocates to the outer leaflet of the endoplasmic reticulum (ER) membrane (26-29). Isoprenylation of the C-terminal CAAX motif of Gγ anchors the nascent Gβγ dimer in the membrane (30, 31). The events underlying the attachment of Gα subunits to the ER membrane and initial association with Gβγ dimers are less well understood. No chaperone or escort factor, such as PhLP-1 or DRIP78, is known to work with the CCT to fold or process G protein α subunits. Once Gα binds to the ER-associated Gβγ dimer and becomes palmitoylated, the intracellularly formed G protein heterotrimers are trafficked to the plasma membrane (32, 33). All members of the Gα$_i$ class of G proteins are also myristoylated irreversibly during translation (34). Myristoylated Gα$_i$ has enhanced affinity for the membrane and increased receptor coupling compared to unmodified Gα$_i$ (35, 36).

Mature heterotrimeric G proteins traffic among the plasma membrane and locales within the cytoplasm through mechanisms that are either dependent or independent of G protein–coupled receptor (GPCR) action (37-40). Trafficking can be vesicle-mediated or diffusive

and, in one case, may be regulated by a cycle of dynamic G protein palmitoylation and depalmitoylation. Depalmitoylated G protein α subunits at the plasma membrane are transported to the Golgi to become repalmitoylated by Golgi-resident aspartate-histidine-histidine-cysteine (DHHC) palmitoyl transferases and are then recycled back to the plasma membrane (41, 42). It is not clear how G proteins are transported by so-called diffusive mechanisms. Factors that might aid or escort G proteins during diffusive shuttling processes have yet to be defined.

To investigate the mechanism by which mammalian Ric-8A and Ric-8B regulate heterotrimeric G protein function in vivo, we created transgenic mice with single deletions of *Ric-8A* or *Ric-8B*. Complete knockouts of these genes resulted in mouse strains that were not viable and died early during embryogenesis [before embryonic day 8.5 (E8.5)]. An independently derived *Ric-8A* knockout mouse was also not viable and exhibited early embryonic lethality and severe gastrulation defects (43). As neither knockout mouse was born, we derived *Ric-8A*$^{-/-}$ or *Ric-8B*$^{-/-}$ embryonic stem (ES) cell lines from viable blastocysts for the purpose of creating cultured cell models with which to study G protein function in the complete absence of Ric-8A or Ric-8B. We observed pleiotropic G protein signaling defects in the *Ric-8A*–null cell lines, which we attributed to a >95% reduction in the steady-state abundances of $G\alpha_i$, $G\alpha_q$, and $G\alpha_{13}$ proteins and partial reductions in the amounts of $G\alpha_s$ and total $G\beta$. The abundance of $G\alpha_s$ alone was reduced ~85% in *Ric-8B*–null cells. In *Ric-8A*–null cells, the translation of $G\alpha_i$ and $G\alpha_q$ proceeded normally, but both nascent G protein α subunits were defective in initial association with the membrane. Much of the nascent $G\alpha$ subunits remained soluble and were rapidly degraded. Thus, we conclude that Ric-8 proteins control G protein abundance and function by acting as molecular chaperones that mediate the initial association of G protein α subunits with an endomembrane.

RESULTS

Ric-8A$^{-/-}$ and *Ric-8B*$^{-/-}$ mouse ES cell lines derived from blastocysts are viable

Transgenic *Ric-8A*– or *Ric-8B*–deleted C57BL/6J mice were created with VelociGene technology (44). The complete *Ric-8A* coding sequence or the first three exons and a portion of the third intron of *Ric-8B* were replaced with *LacZ* expression cassettes under the control of the endogenous *Ric-8* promoters (fig. S1). Homozygous *Ric-8A*$^{-/-}$ or *Ric-8B*$^{-/-}$ mice were not born and exhibited lethality before E8.5 (*n* > 100 mice). Heterozygote mice of each strain were reproductive and had no obvious defects. Fifty-three and 49 preimplantation blastocysts (chemically delayed from E3.5 to E6.5) were harvested from *Ric-8A*$^{+/-}$ or *Ric-8B*$^{+/-}$ intercrosses and grown in culture. Viable inner cell masses were detached and subcultured to enable outgrowth of mouse ES (mES) cell lines. Those surviving derivation resulted in four *Ric-8A*$^{+/+}$, nine *Ric-8A*$^{+/-}$, three *Ric-8A*$^{-/-}$, one *Ric-8B*$^{+/+}$, three *Ric-8B*$^{+/-}$, and seven *Ric-8B*$^{-/-}$ viable mES cell lines as determined by genomic polymerase chain reaction (PCR)–based genotyping (fig. S1). *Ric-8A* and *Ric-8B* were not required for embryonic development of viable blastocysts, placing the timing of embryonic death between E4 and E8.5 for both gene deletions. No obvious morphological differences were observed among mES cell lines cultured on mitotically inactivated mouse embryonic fibroblasts (MEFs) or in feeder-free culture (Fig. 1A). *Ric-8A* and *Ric-8B* promoters were active in mES cell colonies. Dose-dependent β-galactosidase activity was observed as a function of *LacZ* reporter gene copy number (Fig. 1A). mES cell colonies of each genotype uniformly expressed the pluripotency marker Oct3/4 (Fig. 1A) (45).

Relative amounts of Ric-8A and Ric-8B were measured by quantitative Western blotting of whole-cell lysates prepared from two independently derived wild-type, *Ric-8A*$^{-/-}$, and *Ric-8B*$^{-/-}$ cell lines. Ric-8A and two Ric-8B isoforms (Ric-8BFL and Ric-8BΔ9) were not

found in the *Ric-8A*$^{-/-}$ or *Ric-8B*$^{-/-}$ cell lines, respectively (Fig. 1B). The amounts of the Ric-8BFL and Ric-8BΔ9 isoforms were increased ~30 and ~80%, respectively, in the *Ric-8A*$^{-/-}$ cells compared to those in wild-type cells, and the amount of actin was reduced by 40%. The amounts of Ric-8A and actin were unchanged in the *Ric-8B*–deleted cells.

Ric-8A and Ric-8B are required to maintain normal amounts of G protein subunits at steady state

We tested the effects of complete ablation of *Ric-8A* or *Ric-8B* on steady-state G protein amounts in crude membrane fractions (150,000*g* pellets, P150) and whole-cell lysates prepared from duplicate wild-type, *Ric-8A*$^{-/-}$, and *Ric-8B*$^{-/-}$ mES cell lines. Equal amounts of total protein (20 μg of P150 fraction and 60 μg of whole-cell lysate) were analyzed by Western blotting with G protein subunit–specific antisera (Fig. 2A). In both *Ric-8A*$^{-/-}$ cell lines, we observed a marked reduction in the amounts of Gα$_{i1/2}$, Gα$_o$, Gα$_q$, and Gα$_{13}$ in the membrane to <5% of those of wild-type cells. The amount of total Gβ (including Gβ$_1$ to Gβ$_4$) was reduced by 40% compared to that in wild-type cells, and the amount of membrane Gα$_s$ was reduced modestly (~20%). The amount of Gα$_s$ protein in the membrane of both *Ric-8B*$^{-/-}$ cell lines was reduced by 85% compared to that of wild-type cells, but the amounts of all other G proteins were similar to those of wild-type cells. In whole-cell lysates from *Ric-8A*$^{-/-}$ or *Ric-8B*$^{-/-}$ cells, the same patterns of overall reduction in the amounts of G proteins were observed, with the exception of Gα$_s$ in the *Ric-8A*$^{-/-}$ cells. The magnitude of the reductions in the amounts of Gα$_o$, Gα$_{13}$, and Gα$_s$ in whole-cell lysates of *Ric-8A*$^{-/-}$ cells was not great as those in the membrane fraction, indicating that the overall defects in G protein abundance were likely a consequence of Ric-8–mediated association of G proteins with the membrane or stabilization of G proteins at the membrane after attainment of membrane residence. In the absence of Ric-8A, some G proteins were partially shifted to the soluble fraction. The amount of polymerized actin (F-actin) was also reduced in the *Ric-8A*$^{-/-}$ cells compared to that in wild-type cells, but no such reduction occurred in the *Ric-8B*–deleted cell lines.

Gα and Gβγ subunit abundances are interdependent (33). We tested whether transient transfection of *Ric-8A*$^{-/-}$ and *Ric-8B*$^{-/-}$ mES cell lines with plasmids encoding FLAG-tagged Gβ$_1$ and Gγ$_2$ subunits would rescue the steady-state deficits in G protein α subunits in these cell lines (fig. S2). In *Ric-8A*$^{-/-}$ cells, transient overexpression of Gβγ restored the amount of Gα$_s$ in crude membranes to that of wild-type cells, but the amount of Gα$_{i1/2}$ was only rescued from 2.2 to 3.5% of that of wild-type cells. We observed similar percentages in the Gβγ-dependent increase in the amounts of membrane-associated Gα$_s$ and Gα$_{i1/2}$ in wild-type cells. In *Ric-8B*$^{-/-}$ cells, the amount of membrane Gα$_{i1/2}$ was increased in response to the increase in Gβγ abundance, but the amount of membrane Gα$_s$ remained reduced at ~6% of that of wild-type cells.

We then performed genetic complementation tests of the *Ric-8A*– or *Ric-8B*–null cell defects. A *Ric-8A*$^{-/-}$ mES cell line made to stably express human *Ric-8A* complementary DNA (cDNA) as a transgene (Tg) did not exhibit the defects in G protein and F-actin abundance that were observed in *Ric-8A*$^{-/-}$ cells, and restored the amounts of Ric-8BFL and Ric-8BΔ9 to amounts similar to those in wild-type cells (Fig. 2B). We could not generate genetically complemented *Ric-8B*$^{-/-}$ cell lines because stable expression of cDNA encoding Ric-8BFL or Ric-8BΔ9 in mES cells seemed to be repressed. The abundance of the mES cell pluripotency marker Oct3/4 in *Ric-8A*$^{-/-}$ cells was 40% greater than that in wild-type cells but was reduced to ~10% above that of wild-type cells upon complementation with *Ric-8A*. The absence of *Ric-8A* may contribute to the increased pluripotent potential of mES cells, a role consistent with observations that the single *ric-8* genes of *C. elegans* and *Drosophila* are required for asymmetric cell division and differentiation (10, 46).

We conducted quantitative PCR analyses comparing the relative abundances of G protein subunit mRNAs in wild-type mES cell lines with those in *Ric-8A*$^{-/-}$ or *Ric-8B*$^{-/-}$ cell lines to test the possibility that Ric-8 proteins regulated G protein abundance through a pretranslational mechanism (Fig. 2C). The relative amounts of Gα_i, Gα_{13}, Gα_q, and Gβ mRNAs remained largely unchanged in the *Ric-8A*–null and *Ric-8B*–null cell lines compared to those in wild-type cells. The abundance of Gα_s mRNA was increased twofold in the *Ric-8A*$^{-/-}$ cell lines compared to that in wild-type cells, perhaps through a compensatory mechanism. A modest increase in the abundance of *Ric-8B* mRNA was observed in the *Ric-8A*$^{-/-}$ cells, which coincided with the increased amounts of Ric-8BFL and Ric-8BΔ9 proteins.

G proteins are reduced in abundance but not absent from the plasma membrane in *Ric-8A*– and *Ric-8B*–null mES cells

To assess the residency of G protein α subunits and G$\beta\gamma$ dimers in the plasma membranes of wild-type, *Ric-8B*$^{-/-}$, and *Ric-8A*$^{-/-}$ cells, we transiently transfected the mES cell lines with plasmids encoding green fluorescent protein (GFP)– or yellow fluorescent protein (YFP)– tagged G protein α subunits and a split YFP pair that reconstituted the G$\beta_1\gamma_7$ dimer (Fig. 3) (47). Analysis of confocal microscopy images revealed that GFP-Gα_i, GFP-Gα_q, YFP-Gα_{sL}, and split YFP-G$\beta_1\gamma_7$ were present in the plasma membranes of *Ric-8A*–deleted cells, but at substantially reduced intensities compared to those in the plasma membranes of transfected wild-type cells. In the *Ric-8A*$^{-/-}$ cell line expressing the *Ric-8A* cDNA, the fluorescence intensities of each expressed G protein in the plasma membrane were restored. In the *Ric-8B*$^{-/-}$ cells, only YFP-Gα_{sL} exhibited a reduced intensity in the plasma membrane. These results were consistent with the patterns of reduced abundances of endogenous G proteins at steady state that were observed earlier (Fig. 2). We conclude that Ric-8 proteins are not essential for the trafficking of overexpressed G protein heterotrimers to the plasma membrane but are indeed necessary to establish or maintain normal amounts of G proteins in the membrane.

The biosynthesis and initial association of G proteins with intracellular membranes are defective in *Ric-8A*$^{-/-}$ mES cells

The reduced abundances of select G protein α subunits in *Ric-8A*– or *Ric-8B*–null cells might be accounted for if Ric-8 proteins functioned as chaperones that escorted nascent G protein α subunits to the membrane, aided the folding of nascent G α subunits, or both. We developed metabolic labeling and coimmunoprecipitation procedures to address the mechanism of synthesis of G protein α subunits and assembly of G protein heterotrimers in *Ric-8A*$^{-/-}$ cells. Wild-type mES cells were first labeled with [^{35}S]methionine and [^{35}S] cysteine for 60 min. Labeled whole-cell lysates were subjected to immunoprecipitation with antiserum (B084) against G$\alpha_{i1/2}$ (48) in the presence of guanosine diphosphate (GDP) or Mg^{2+} and guanosine 5′-*O*-(3′-thiotriphosphate) (GTP-γ-S). G$\beta\gamma$ is dissociated from Gα when the latter becomes bound to GTP-γ-S. The immunoprecipitates were analyzed by Western blotting with antiserum against G$\alpha_{i1/2}$ and antiserum (U49) against Gβ_1 (48), or were subjected to autoradiography. When GTP-γ-S was included, Gβ_1 was not present in the G$\alpha_{i1/2}$ immunoprecipitates, and two prominent ~37-kD bands were also absent on the autoradiograph (Fig. 4A). We concluded that these bands represented two or more endogenous Gβ isoforms that bound to endogenous G$\alpha_{i1/2}$.

We next measured the time course of G$\alpha_{i1/2}$ synthesis and its association with nascent G$\beta\gamma$ subunits in the *Ric-8A*$^{-/-}$ and genetically complemented mES cell lines. The mES cells were metabolically pulse-labeled for up to 1 hour and subjected to immunoprecipitation with antiserum against G$\alpha_{i1/2}$ at the indicated times (Fig. 4B). G$\alpha_{i1/2}$ was synthesized at equivalent rates in *Ric-8A*$^{-/-}$ cells stably expressing pcDNA or the human *Ric-8A* cDNA

(Tg), showing that the translation of G protein α subunits was not affected by the loss of *Ric-8A*; however, we uncovered other differences between these cell lines. In the *Ric-8A$^{-/-}$* cells, two Gα$_i$ species of different apparent molecular masses were reproducibly recovered from the Gα$_{i1/2}$ immunoprecipitates over the course of the pulse labeling study, whereas only one species of lower apparent mobility was recovered from the *Ric-8A*–complemented *Ric-8A$^{-/-}$* cells (Fig. 4B and fig. S3). At 60 min of cell labeling, the ratio of the two Gα$_{i1/2}$ species approached 1:1 in the *Ric-8A$^{-/-}$* cells. Before this, most of the nascent Gα$_{i1/2}$ had a higher apparent mobility. Gα$_i$ subunits are myristoylated cotranslationally, and the modified and unmodified forms can be resolved by SDS–polyacrylamide gel electrophoresis (SDS-PAGE) (1, 34, 49). We tested whether these might be the two forms of nascent Gα$_i$ observed in *Ric-8A$^{-/-}$* cells by examining the SDS-PAGE mobilities of transiently expressed Glu-Glu–tagged wild-type Gα$_{i1}$ or the myristoylation-defective mutant Gα$_{i1}$ G2A (fig. S3). Nascent, wild-type Glu-Glu–tagged Gα$_{i1}$ migrated distinctly faster than did Glu-Glu–tagged G2A Gα$_{i1}$, as was expected for the myristoylated protein; however, a wild-type Glu-Glu–tagged Gα$_{i1}$ doublet could not be resolved in samples from *Ric-8A$^{-/-}$* cells that were subjected to immunoprecipitation with antibody against Glu-Glu despite the clear resolution of Glu-Glu–tagged wild-type Gα$_{i1}$ and Glu-Glu–tagged G2A Gα$_{i1}$ in adjacent lanes. This suggested that the endogenous nascent Gα$_i$ doublet observed in the *Ric-8A$^{-/-}$* cell lines might not correspond to the myristoylated and unmodified forms of the protein. Gα$_i$ may be subject to a hitherto unknown modification during early biosynthesis that is revealed when Ric-8A is not present.

Next, we investigated the temporal association of newly synthesized Gα$_{i1/2}$ and Gα$_q$ with cell membranes and the formation of G$_i$ heterotrimers. *Ric-8A$^{-/-}$* cells expressing *Ric-8A* (Tg) or sham cDNA were pulse-labeled for 10 min and were fractionated into soluble and crude membranes by centrifugation at different chase times (0, 15, and 30 min). Gα$_{i1/2}$ or Gα$_q$ was immunoprecipitated from the subcellular fractions and visualized with coimmunoprecipitating Gβγ by autoradiography (Fig. 4C). Gβγ was not efficiently coimmunoprecipitated with the antiserum against Gα$_q$. At each time of chase, ~45 to 50% of the newly made Gα$_{i1/2}$ and ~90% of the newly made Gα$_q$ was defectively retained in the soluble fraction of *Ric-8A$^{-/-}$* cells. The reduced portion of nascent Gα$_{i1/2}$ that fractionated with membranes in the *Ric-8A$^{-/-}$* cells became bound to Gβγ with high stoichiometry (~1:1). In the *Ric-8A*–complemented *Ric-8A$^{-/-}$* cells, membrane-associated nascent Gα$_{i1/2}$ reached a stoichiometry of only ~0.4 to 0.6 mol of Gβγ per mole of Gα$_{i1/2}$. These results are consistent with the Gα$_i$:Gβγ stoichiometry measurements made in the whole-cell pulse-labeling experiment (Fig. 4B), but were unexpected given the defects in the steady-state amounts of Gα$_{i1/2}$ and total Gβγ in the *Ric-8A$^{-/-}$* cells. We speculate that cotranslationally myristoylated Gα$_i$ is better able to complete initial endomembrane association in the absence of Ric-8A than are other classes of G protein α subunits because these other α subunits are not myristoylated. Although the overall abundance of nascent membrane-bound Gβγ may also be reduced in *Ric-8A$^{-/-}$* cells, the availability of free Gβγ sites to accept nascent, myristoylated Gα$_i$ may actually be higher because of the bulk reduction in the amounts of all membrane Gα subunits.

The defect in the association of Gα$_q$ with membranes was more marked than that of Gα$_{i1/2}$ in *Ric-8A$^{-/-}$* cells, and we reasoned that a lengthened kinetic delay might account for this defect. We immunoprecipitated Gα$_q$ with two polyclonal Gα$_q$-specific antisera (Z808 and Z811) from subcellular fractions of cells pulse-labeled for 2 hours (which approximated the steady-state condition) (Fig. 4D). Nearly all of the Gα$_q$ was membrane-associated in *Ric-8A*–complemented *Ric-8A$^{-/-}$* mES cells, but a reduced quantity was present predominantly in the cytosol of *Ric-8A$^{-/-}$* cells. Unlike Gα$_{i1}$, nascent Gα$_q$ is not cotranslationally lipidated and it has a stringent requirement for Ric-8A for its initial membrane association.

Enhanced G protein turnover accounts for reduced steady-state amounts in *Ric-8A*–null mES cells

The large Ric-8A–dependent reductions in the steady-state amounts of Gα and total Gβ could be explained if the nascent Gα subunits that did not associate with the membrane were rapidly degraded. We measured the protein turnover rates of endogenous $Gα_{i1/2}$, $Gα_q$, and $Gβ_1$ in *Ric-8A*$^{-/-}$ cells expressing *Ric-8A* (Tg) or sham cDNA. Cells were pulse-labeled for 60 min and chased over a 24-hour time course. $Gα_{i1/2}$, $Gα_q$, $Gβ_1$, Ric-8A, and γ-tubulin were individually immunoprecipitated and visualized by SDS-PAGE or autoradiography (Fig. 5). The turnover rates of $Gα_{i1/2}$ and $Gα_q$ were enhanced markedly in the *Ric-8A*–deleted cells, with half-lives ($t_{1/2}$) of $2.6 ± 0.6$ and $1.7 ± 0.2$ hours compared to $16.5 ± 0.7$ and $18 ± 0.9$ hours, respectively, when *Ric-8A* was expressed. $Gβ_1$ was also degraded faster in *Ric-8A*–deleted cells with a $t_{1/2}$ of $3.8 ± 0.7$ hours compared to $16.1 ± 2.7$ hours in cells in which *Ric-8A* was expressed. An unrelated control protein, γ-tubulin was degraded with similar kinetics in both cell lines, and the $t_{1/2}$ of Ric-8A turnover was $16.2 ± 1.1$ hours. In the *Ric-8A*$^{-/-}$ cells, the substantial delay in $Gβ_1$ turnover in comparison to that of Gα ($\Delta t_{1/2}$ ~1.2 to 2.1 hours) may reflect the higher stability of $Gβ_1$ compared to that of Gα, or it could delineate the sequence of events in the turnover of these proteins in the absence of Ric-8A.

Basal and β-adrenergic–stimulated AC activities are attenuated in *Ric-8A*$^{-/-}$ and *Ric-8B*$^{-/-}$ mES cells

G protein allosteric modulators of AC enzymes include the stimulatory $Gα_s$ protein and the inhibitory $Gα_i$ protein, as well as Gβγ-specific regulation of AC isoforms (50). *Ric-8A* deletion resulted in reduced amounts of $Gα_i$ and total Gβ proteins and modestly lowered amounts of membrane-bound $Gα_s$, whereas deletion of *Ric-8B* affected the abundance of $Gα_s$ alone. We measured total AC activity in duplicate wild-type and *Ric-8*–null mES cell lines. Basal amounts of adenosine 3′,5′-monophosphate (cAMP) in *Ric-8B*$^{-/-}$ and *Ric-8A*$^{-/-}$ were lower than that in wild-type cells (Fig. 6A). Stimulation of wild-type, *Ric-8A*$^{-/-}$, and Ric-8B$^{-/-}$ cells with a β-adrenergic receptor (β-AR) agonist produced a similar result. The maximal amounts of isoproterenol-induced cAMP were lower in *Ric-8B*–null cells than in wild-type cells, but were most reduced in *Ric-8A*–null cells. Isoproterenol was equipotent in each of the three cell types [median effective concentration (EC_{50}) range of ~410 to 515 nM], suggesting that the observed dysregulation of cAMP accumulation did not occur at the level of β-ARs in the absence of Ric-8A or Ric-8B (Fig. 6B). The defects were manifested in the initial phase of cAMP accumulation because a saturating concentration of isoproterenol (10 μM) in the presence of phosphodiesterase inhibitors stimulated wild-type cells to accumulate cAMP at the fastest rate (100 fmol/min) and *Ric-8A*$^{-/-}$ cells to accumulate cAMP at the slowest rate (38 fmol/min), whereas *Ric-8B*$^{-/-}$ cells produced cAMP at an intermediate rate (58 fmol/min) (Fig. 6C). Treatment of mES cells with forskolin, a direct activator of AC, recapitulated the results observed with isoproterenol. Forskolin potency was largely unaffected by *Ric-8A* or *Ric-8B* deletion, but the maximal response to forskolin was blunted the most in *Ric-8A*$^{-/-}$ cells and to an intermediate extent in *Ric-8B*$^{-/-}$ cells (Fig. 6D and fig. S4). We observed the known synergism between forskolin and isoproterenol in each cell type, but similar overall patterns of cAMP accumulation persisted.

The dose-dependent relationship between isoproterenol and cAMP accumulation in the *Ric-8A*$^{-/-}$ mES cell line genetically complemented with *Ric-8A* (Tg) or expressing sham cDNA showed that stable *Ric-8A* expression rescued the defect in cAMP accumulation in *Ric-8A*–null cells (Fig. 6E). In summary, basal as well as hormone- and forskolin-stimulated cAMP amounts were most depressed in *Ric-8A*$^{-/-}$ cell lines and to an intermediate extent in the *Ric-8B*$^{-/-}$ cell lines. The simplest interpretation of these reductions in the amounts of cAMP in *Ric-8B*$^{-/-}$ cells is that they are a result of the ~85% loss in the abundance of the AC activator, $Gα_s$. It is not intuitively clear why cAMP concentrations were further

depressed in *Ric-8A*–null cells because these cells expressed substantially more $G\alpha_s$ and less $G\alpha_i$ than did the *Ric-8B*$^{-/-}$ cells. The pronounced reduction in the amount of total G proteins, particularly steady-state $G\beta\gamma$ abundance in the *Ric-8A*$^{-/-}$ cells, may have contributed to the reduced total AC activities. Alternatively, misregulation at the level of AC enzyme(s) or combinatorial effects thereof with the reduced G protein amounts seems likely.

Lysophosphatidic acid receptor–dependent and Rho-dependent modulation of F-actin amounts and structure are perturbed in *Ric-8A*–null mES cells

Lysophosphatidic acid (LPA) receptors activate $G_{12/13}$ family G proteins, whose $G\alpha_{12}$ and $G\alpha_{13}$ subunits in turn bind to p115 Rho GEFs to activate Rho family guanosine triphosphatases (GTPases) (51). Activated Rho signals to alter the actin cytoskeleton and the adhesive properties of cells. Ric-8A stimulates guanine nucleotide exchange on $G\alpha_{13}$ (1), and we found that it was required for optimal $G\alpha_{13}$ abundance (Fig. 2). Whole-cell actin and precipitable actin (F-actin) were also reduced 40 and 70%, respectively, in *Ric-8A*$^{-/-}$ cells, but not in *Ric-8B*$^{-/-}$ cells (Figs. 1B and 2A). To test whether the defect in F-actin was attributed to aberrant $G_{12/13}$-mediated regulation of Rho signaling, we measured basal (continuous serum only) and LPA-stimulated amounts of Rho-GTP by glutathione *S*-transferase (GST)–Rhotekin pull-down assays in *Ric-8A*$^{-/-}$ mES cells that stably expressed *Ric-8A* (Tg) or sham cDNA (Fig. 7A). We found that the total amounts of Rho in these cells were equivalent, but that the basal amount of Rho-GTP was markedly reduced in the *Ric-8A*$^{-/-}$ cells compared to that in the *Ric-8A*–complemented *Ric-8A*$^{-/-}$ cells. The percentage increase in LPA-stimulated production of Rho-GTP over basal amounts was similar in both cell types, but LPA-induced Rho-GTP amounts were substantially higher in *Ric-8A*$^{-/-}$ cells than in *Ric-8A*$^{-/-}$ cells complemented with *Ric-8A* cDNA.

We then transiently transfected the cell lines with plasmids encoding dominant-negative or constitutively active RhoA proteins and incubated the cells with rhodamine-phalloidin to visualize actin microfilaments and filopodia by microscopy (Fig. 7B). Sham-transfected *Ric-8A*$^{-/-}$ cells had reduced amounts of actin microfilaments and filopodia-like structures compared to those of *Ric-8A*$^{-/-}$ cells stably expressing *Ric-8A* cDNA (Tg). Expression of dominant-negative RhoA reduced the numbers of phalloidin stained actin structures in the *Ric-8A*–expressing cells, whereas constitutively active RhoA increased the numbers of such structures in both cell types. Fractionation of total soluble G-actin from precipitable F-actin corroborated the microscopic analysis. The amounts of G-actin were unchanged, but substantially less F-actin was present in the *Ric-8A*–null cells than was in the Ric-8A–expressing cells (Fig. 7C). Constitutively active RhoA restored the deficit in F-actin observed in *Ric-8A*$^{-/-}$ cells. Signaling downstream of Rho was not perturbed in *Ric-8A*$^{-/-}$ cells, which implied that the misregulation of the actin cytoskeleton was at the level of Rho activation. Likely candidates of this misregulation include $G\alpha_{12/13}$ and $G\alpha_q$ subunits because these G proteins activate Rho GEFs and were reduced in abundance >95% in *Ric-8A*$^{-/-}$ cells relative to wild-type cells.

DISCUSSION

Here, we found that Ric-8 GEFs were molecular chaperones that directed the initial association of nascent G protein α subunits with intracellular membranes. In cultured mES cell lines with deletions of *Ric-8A* or *Ric-8B*, we observed marked reductions in the steady state abundances of G protein α subunits. In *Ric-8A*–null cells, substantial portions of newly synthesized α subunits remained soluble and were degraded rapidly. Weak plasma membrane staining of transiently expressed G protein subunits persisted in the Ric-8–deficient cells. The basic scheme of the plasma membrane trafficking pathway remained

intact for the small portion of nascent G proteins that became associated with intracellular membranes.

Reduced amounts of G proteins in *Ric-8A–* or *Ric-8B–*null cells resulted in GPCR signaling defects. We examined AC activity because control of this effector system by $G\alpha_i$ and $G\alpha_s$ is well characterized, and Ric-8A and Ric-8B act with exclusivity as GEFs and binding partners for these respective G proteins. *Ric-8A–*null cells had the lowest basal, β-AR agonist–, and forskolin-stimulated AC activities. *Ric-8B–*null cells had only partially depressed AC activities despite having the least amount of $G\alpha_s$. The greater loss of total AC activity in *Ric-8A–*null cells was unexpected and may have been a consequence of the substantial partial loss of total Gβ, which would reduce the efficiency of functional coupling between the GPCR and $G\alpha_s$. Misregulation of additional signaling inputs, including reductions in the abundance or function of AC, is a plausible possibility in *Ric-8–*deleted cells and merits further examination. It is clear that the near-complete loss of $G\alpha_i$ class subunits in *Ric-8A–*null cells and thus the relief of tonic $G\alpha_i$-mediated inhibition of AC was far less consequential toward total cellular AC activities than were the 20 and 40% reductions in the amounts of membrane $G\alpha_s$ and total Gβγ, respectively, in addition to any potential misregulation of AC that might have occurred.

The cause of the reduction in the amount of Gβγ in *Ric-8A–*null, but not *Ric-8B–*null, cells was secondary to the reduced bulk steady-state amounts of Gα subunits (the $G\alpha_i$ class being the most abundant). In HeLa cells, short interfering RNA (siRNA)–mediated silencing of $G\alpha_{i1}$, $G\alpha_{i2}$, and $G\alpha_{i3}$ resulted in a 50% reduction in the amount of total Gβ (52). Extending this logic, the 20% reduction in the amount of membrane $G\alpha_s$ in *Ric-8A–*null cells would be a tertiary consequence of the ~40% loss of the total Gβ pool, because Ric-8A is not a GEF for $G\alpha_s$ and does not bind to this subunit. Furthermore, the deficit in membrane $G\alpha_s$ was rescued by overexpression of $G\beta_1$ and $G\gamma_2$ in *Ric-8A$^{-/-}$* cells, but not in *Ric-8B$^{-/-}$* cells. In summary, the primary defects in G protein α subunit abundance in *Ric-8A–* or *Ric-8B–*deleted mES cells are consistent with the known enzymatic and binding preferences that Ric-8A and Ric-8B have for distinct subsets of the G protein α subunit classes, with Ric-8A binding to $G\alpha_i$, $G\alpha_q$, and $G\alpha_{12/13}$, whereas Ric-8B binds to $G\alpha_s$.

Our study prompts the question of how the GEF activity of Ric-8 regulates the membrane attachment of newly synthesized Gα subunits. We propose that Ric-8 GEF activity may not necessarily (or always) be for the purpose of producing activated Gα-GTP to evoke signaling outputs (1). Rather, Ric-8 may make use of the G protein guanine nucleotide switch as a means to become dissociated from Gα. Ric-8 proteins preferentially bind to nucleotide-free G protein α subunits, and they become dissociated upon binding of GTP to Gα. Nascent Gα subunit protein chains that emerge from ribosomes are not bound to guanine nucleotide until they fold properly and develop a guanine nucleotide–binding pocket. If Ric-8 binds to a G protein α subunit that is emerging from the ribosome, it could assist the folding or presentation of the unfolded Gα protein chain to the CCT (Fig. 8). Analogous to the actions of PhLP-1 and Gβ, Ric-8 could form a ternary complex with Gα and CCT during folding of the G protein α subunit (Fig. 8) and subsequently act as the escort chaperone to shuttle the nascent, nucleotide-free G protein α subunit to an ER-docking site (Fig. 8). At the ER, Ric-8 could be stimulated to induce nucleotide exchange and release free Gα-GTP onto the membrane (Fig. 8). Subsequent GTP hydrolysis by Gα may occur intrinsically or may be aided by the GTPase-activating activity of an endomembrane-specific regulator of G protein signaling (RGS) protein (Fig. 8). Gα-GDP would then be primed to bind to free Gβγ and assemble a nascent G protein heterotrimer before it is targeted to the plasma membrane.

Here, we have defined a specific role for Ric-8 proteins as molecular chaperones that regulate G protein biosynthesis. This role provides an explanation of how Ric-8 proteins seemingly regulate diverse G protein signaling outputs in worms, flies, and mammals. Other roles for Ric-8–mediated regulation of G proteins in cells should not be overlooked. Ric-8A and *C. elegans* RIC-8 are recruited to the growing mitotic spindle and may work with $G\alpha_i$ and GPR/GoLoco-containing proteins to regulate spindle positioning during cell division (9, 12). Documented localization of Ric-8A at the spindle is not intuitively consistent with an exclusive role for Ric-8A as a chaperone that regulates the biosynthesis of G protein α subunits. A study found that Ric-8B is recruited to the plasma membrane upon chronic stimulation with high concentrations of GPCR agonists (53). In that study, the plasma membrane–docking site for Ric-8B was not shown but was inferred to be G protein α subunits dissociated from $G\beta\gamma$ dimers. Mature G proteins are thought to transit diffusively among the plasma membrane and endomembranes. Perhaps, additional roles for Ric-8 proteins as escort chaperones for G protein α subunits in trafficking pathways distinct from initial biosynthesis exist and remain to be explored.

MATERIALS AND METHODS

Reagents, antibodies, and plasmids

Rabbit polyclonal antiserum 2414 against Ric-8B was produced by Capralogics Inc., using purified full-length Ric-8B protein as an immunogen. Rabbit polyclonal antiserum against Ric-8A was used to detect Ric-8A protein (54). G protein subunit–specific antisera were used to detect $G\alpha_{i1/2}$ (BO84), $G\beta_{1-4}$ (B600) (55), $G\alpha_o$ (S214), $G\alpha_s$ (584), $G\beta_1$ (U49) (48), $G\alpha_q$ (WO82, Z811, and Z808) (56, 57), and $G\alpha_{13}$ (B860) (58). Antibodies against actin, α-tubulin, γ-tubulin, and Oct3/4 were from Sigma-Aldrich Inc. Antibody against glyceraldehyde-3-phosphate dehydrogenase (GAPDH) was from Santa Cruz Biotechnology Inc. Antibody against Rho (clone 55) was from Millipore. cDNA encoding human *Ric-8A* was subcloned by linker-based PCR from HeLa cell cDNA into the Nhe I and Not I sites of pcDNA3.1/Hygro or pcDNA3.1/Neo. Plasmids encoding $G\alpha_i$-GFP and $G\alpha_q$-GFP were gifts from A. Smrcka and S. Malik. Plasmids encoding $G\alpha_{sL}$-YFP, YFP–N-β_1, and YFP–C-γ_7 were gifts from C. Berlot (47, 59). cDNAs encoding human Glu-Glu–tagged $G\alpha_{i1}$, FLAG-$G\beta_1$, $G\gamma_2$, RhoT19N, and RhoG12V in pcDNA3.1/Neo (Invitrogen) were obtained from the S&T cDNA Resource Center. Sequences encoding wild-type and Glu-Glu–tagged G2A $G\alpha_{i1}$ were amplified by PCR (using a mutant sense strand primer to create G2A) and subcloned into pcDNA3.1/Hygro (Invitrogen).

Engineering of mouse *Ric-8A*– and *Ric-8B*–null alleles

Targeted mES cells harboring null alleles of *Ric-8A* (VelociGene ID: VG #546) or *Ric-8B* (VelociGene ID: VG#547) were generated with VelociGene technology (44). Bacterial artificial chromosomes (BACs) containing mouse genomic DNA encompassing *Ric-8A* or *Ric-8B* were selected by a PCR-based screen from a 129/Svj mouse genomic DNA BAC library (Incyte). The BAC ID for *Ric-8A* was from BAC ES release 2: 109m11 and contained ~135 kb of genomic DNA. The BAC ID for *Ric-8B* was from BAC ES release 2: 292o14 and contained ~170 kb of genomic DNA. To generate the targeting vectors, we replaced a 4961–base pair (bp) region of the *Ric-8A* locus consisting of the entire coding sequence with a transmembrane domain–LacZ/Neomycin phosphotransferase (TM-LacZ/Neo)–encoding cassette by bacterial homologous recombination (BHR) (60-63). An ~30,689-bp region spanning the first three exons and a portion of the third intron of the *Ric-8B* locus was also replaced with this cassette. In preparation for targeting, the modified BACswere subjected to restriction digest with Not I to generate linear targeting vectors with BAC homology arms of about 40 and 95 kb, for *Ric-8A*, or 50 and 100 kb, for *Ric-8B*, flanking the TM-LacZ/Neo cassettes. The ES line F1H4, a C57BL/6-129SvJ hybrid, was

electroporated with the linearized constructs. 288 *Ric-8A* and 288 *Ric-8B* ES cell clones were selected and genotyped by loss-of-allele (LOA) assays (44). Seventeen of 288 *Ric-8A* clones and 8 of 288 *Ric-8B* clones were targeted, indicating targeting frequencies of 5.9 and 2.8%, respectively. Mice were generated by microinjection of the targeted ES cells into C57BL/6 blastocysts and backcrossed to C57BL/6 mice.

Derivation and culture of mES cell lines

Three- to 5-week-old *Ric-8A*$^{+/-}$ or *Ric-8B*$^{+/-}$ (C57BL/6) mice were superovulated by intraperitoneal injection of 5 IU of pregnant mare serum gonadotropin (PMSG), whichwas followed 48 hours later by injection of 5 IU of human chorionic gonadotropin (hCG) (Sigma-Aldrich). Mice were mated and, 48 hours after fertilization, were injected intraperitoneally with 0.1 mg of tamoxifen and subcutaneously with 3 mg of medroxyprogesterone acetate (Sigma-Aldrich) to prevent blastocyst implantation. After 4 days (delayed ~E6.5), pregnant mice were killed, uteri and oviducts were dissected, and blastocysts were flushed out with Dulbecco's modified Eagle's medium (DMEM) buffered with 20 mM Hepes (pH 7.4) (Invitrogen). Blastocysts were cultured individually on 0.1% gelatin–coated plates in RESGRO medium (Millipore). After 2 days of growth, inner cell masses were mechanically detached and subcultured in RESGRO medium. Derived mES cell lines were maintained in ES cell medium [DMEM containing 15% fetal bovine serum (FBS), 1× nonessential amino acid mixture (Invitrogen), 0.1 mM β-mercaptoethanol, and recombinant leukemia inhibitory factor (LIF) (10 μg/ml; Millipore)]. MEFs were isolated from E14.5 wild-type C57BL/6 mouse embryos as described previously (64). To assess β-galactosidase activity in stem cells, we washed the cells with phosphate-buffered saline (PBS), fixed them with 0.2% glutaraldehyde, and stained them in 2 μM MgCl$_2$, 4 μM ferrous cyanide, 4 μM ferric cyanide, and X-galactosidase (0.5 mg/ml) in PBS at 37°C for up to 2 hours.

AC assays

In standard assays, 4×10^4 ES cells were seeded per well in 96-well plates 24 hours before commencement of the assay. For the basal cAMP cell titration experiment, 1×10^4 to 75×10^4 cells were seeded per well. The medium was exchanged with DMEM containing 20 mM Hepes (pH 7.4), 0.1 mM isobutylmethylxanthine (IBMX), 0.1 mM rolipram, and 0.1% bovine serum albumin (BSA) for all experiments. For the isoproterenol time course experiment, cells were incubated with isoproterenol (10 μM) for 0 to 5 min at 22°C. For the isoproterenol dose-response experiments, cells were incubated with isoproterenol (0 to 10 μM) for 2 min at 22°C. To measure the combined effects of forskolin and isoproterenol, we incubated cells with isoproterenol (100 nM) with or without soluble forskolin (50 μM, Tocris Bioscience) for 5 min at 22°C. Reactions were quenched with the LANCE cAMP Detection Kit lysis reagent (PerkinElmer), and the accumulated cAMP was measured according to the manufacturer's instructions with a Victor 3V plate reader (PerkinElmer). Signals were measured at 615 and 665 nm.

Measurements of Rho-GTP and F-actin abundance

Cells were either left untreated or treated with oleoyl-ʟ-α-lysophosphatidic acid (LPA, 10 μM; Avanti Polar Lipids Inc.) for 3 min and lysed in the lysis/binding/wash buffer supplied in the EZ-Detect Rho Activation Kit (Pierce). Total protein was quantified by Amido Black Protein Assay (65). Equivalent samples were supplemented with GST-Rhotekin RBD, and Rho-GTPwas isolated according to the manufacturer's instructions (Pierce). Total Rho and Rho-GTP were visualized by Western blotting analysis with an antibody against Rho that detected Rho protein (clone 55, Millipore). ES cells grown on gelatin-coated glass were rinsed in PBS, fixed with 4% paraformaldeyhyde (PFA), blocked with 5% BSA in PBS, and

stained with rhodamine-phalloidin (0.25 U/ml; Invitrogen) and 4′,6-diamidino-2-phenylindole (DAPI) (0.1 µg/ml; Invitrogen). F-actin structures and nuclei were imaged by confocal microscopy with a 60× oil immersion objective [numerical aperture (NA) = 1.35]. For fractionation of F-actin and G-actin, cells were lysed by nitrogen cavitation (Parr Industries), and lysates were centrifuged at 150,000g for 60 min. Laemmli sample buffer was added to the soluble and precipitate fractions. Samples were resolved by SDS-PAGE and analyzed by Western blotting with an antibody against actin (Sigma-Aldrich).

Quantitative PCR analysis

Total RNA was isolated from feeder-free ES cells with the RNA queous RNA isolation kit (Ambion). RNA was converted to cDNA with a Transcriptor First Strand cDNA Synthesis Kit (Roche). PCR assays (each containing 20 µl of reaction volume) were performed in triplicate with an ABI Prism 7000 Real-Time PCR cycler (Invitrogen) and consisted of 1 µg of cDNA, uniquely designed combinations of TaqMan probes and primers (Roche Universal Probe Library Assay Design Center), and FastStart Universal Probe Master Mix with ROX (Roche). The relative amounts of mRNAs in the *Ric-8* knockout cell line compared to those in wild-type cells were calculated with the $\Delta\Delta C_t$ method (66) and an actin reference gene TaqMan assay. All TaqMan assays were verified to be >85% efficient.

Metabolic labeling and immunoprecipitations

Feeder-free ES cells were grown in gelatin-coated dishes and starved in cysteine- and methionine-free DMEM (Mediatech Inc.) supplemented with 2 mM L-glutamine, 1× nonessential amino acid mixture (Invitrogen), 0.1 mM β-mercaptoethanol, and 15% dialyzed FBS (Invitrogen) for 20 to 45 min. Cells were metabolically pulse-labeled at 37°C in this medium supplemented with L-[^{35}S]cysteine and L-[^{35}S]methionine (200 to 300 µCi/ml; EXPRE^{35}S^{35}S Protein Labeling Mix, PerkinElmer) for the indicated times. Cells subjected to chase were washed once and incubated at 37°C in chase medium (ES cell medium without LIF, supplemented with 1 mM L-cysteine and 1 mM L-methionine). For biosynthesis and coimmunoprecipitation experiments, labeled cells (from ~90% confluent 60-mm dishes) were washed with ice-cold PBS and solubilized in PBS containing 2% NP-40, 1 µM GDP, and a mixture of protease inhibitors [phenylmethylsulfonyl fluoride (23 µg/ml), N_α-tosyl-L-lysine-chloromethyl ketone (21 µg/ml), L-1-*p*-tosylamino-2-phenylethyl-chloromethyl ketone (21 µg/ml), leupeptin (3.3 µg/ml), and lima bean trypsin inhibitor (3.3 µg/ml) (Sigma-Aldrich)]. Clarified detergent lysates were incubated with antisera for 18 hours at 4°C followed by incubation with Protein A–Agarose (Roche) for 4 hours at 4°C. Protein A–captured antibody-antigen complexes were solubilized in Laemmli sample buffer and resolved on 12% tris-glycine-SDS gels. Gels were dried and subjected to autoradiography. For subcellular fractionation pulse-chase labeling experiments, labeled cells (from two ~90% confluent 10-cm dishes) were lysed by nitrogen cavitation in fractionation lysis buffer (PBS containing 1 mM EDTA, 1 µM GDP, and protease inhibitor mixture). The postnuclear 500g supernatants were centrifuged at 150,000g for 30 min. Soluble fractions were supplemented with 1% sodium cholate and 1% NP-40, precleared with Protein A–Agarose, and subjected to immunoprecipitation as described earlier. Crude membrane fractions were dounce-homogenized in fractionation lysis buffer containing 1% sodium cholate and 1% NP-40 and rotated for 10 min at 22°C to extract proteins. The membrane extracts were clarified by centrifugation and subjected to immunoprecipitation. For protein turnover measurements, metabolically labeled cells (from ~90% confluent 60-mm dishes) were lysed in cholate lysis buffer [40 mM tris (pH 7.7), 1 mM EGTA, 2 mM MgCl$_2$, 1% sodium cholate, BSA (100 µg/ml), and protease inhibitor mixture] and clarified by centrifugation at 21,000g. To immunoprecipitate partially denatured individual antigens (Gα$_{i1/2}$, Gα$_q$, Gβ$_1$, Ric-8A, and γ-tubulin), we added SDS (0.5%) and Triton X-100 (1%) and precleared the supernatants with Protein A–Agarose before immunoprecipitation.

Cell imaging

For Oct3/4 immunofluorescence experiments, cells seeded on coverslips were rinsed twice with PBS and fixed with 4% PFA in PBS for 20 min at 22°C. Fixed cells were treated with PBS containing 0.1% Triton X-100, blocked in 5% BSA in PBS, and incubated with antibody against Oct3/4. Cells were washed and incubated with Alexa Fluor 568–conjugated antibody against mouse antibody (Invitrogen). Washed cells were stained with DAPI, mounted, and imaged with a Nikon TE200 inverted microscope with 10× or 20× objective lenses coupled to a monochrometer-based epifluorescence illumination system (TILL Photonics). Excitation was performed at 405 and 568 nm, and images were captured with a high-speed, digital charge-coupled device (CCD) camera (TILL Photonics). To image live cells that were transfected with plasmids encoding fluorescently tagged G protein subunits, we exchanged the cell medium with Hank's balanced salt solution (HBSS). Cells were imaged on an Olympus BX61WI upright microscope coupled to an Olympus Fluoview 1000 multiphoton/confocal (FV1000MP) microscope equipped with a suite of diode and gas lasers. Imaging was performed with a 60× water immersion objective (NA = 0.9).

Statistical analysis

Error bars represent the SEM for at least three independent experiments as indicated throughout. Two-tailed unpaired t tests with confidence intervals of 95% were conducted as indicated.

Supplementary Material

Refer to Web version on PubMed Central for supplementary material.

Acknowledgments

REFERENCES AND NOTES

1. Chan P, Gabay M, Wright FA, Tall GG. Ric-8B is a GTP-dependent G protein α_s guanine nucleotide exchange factor. J Biol Chem. 2011; 286:19932–19942. [PubMed: 21467038]

2. Tall GG, Krumins AM, Gilman AG. Mammalian Ric-8A (synembryn) is a heterotrimeric Gα protein guanine nucleotide exchange factor. J Biol Chem. 2003; 278:8356–8362. [PubMed: 12509430]

3. Miller KG, Alfonso A, Nguyen M, Crowell JA, Johnson CD, Rand JB. A genetic selection for *Caenorhabditis elegans* synaptic transmission mutants. Proc Natl Acad Sci U S A. 1996; 93:12593–12598. [PubMed: 8901627]

4. Miller KG, Emerson MD, McManus JR, Rand JB. RIC-8 (synembryn): A novel conserved protein that is required for $G_q\alpha$ signaling in the *C. elegans* nervous system. Neuron. 2000; 27:289–299. [PubMed: 10985349]

5. Miller KG, Rand JB. A role for RIC-8 (synembryn) and GOA-1 ($G_o\alpha$) in regulating a subset of centrosome movements during early embryogenesis in *Caenorhabditis elegans*. Genetics. 2000; 156:1649–1660. [PubMed: 11102364]

6. Reynolds NK, Schade MA, Miller KG. Convergent, RIC-8-dependent Gα signaling pathways in the *Caenorhabditis elegans* synaptic signaling network. Genetics. 2005; 169:651–670. [PubMed: 15489511]

7. Afshar K, Willard FS, Colombo K, Johnston CA, McCudden CR, Siderovski DP, Gönczy P. RIC-8 is required for GPR-1/2-dependent Gα function during asymmetric division of *C. elegans* embryos. Cell. 2004; 119:219–230. [PubMed: 15479639]

8. Couwenbergs C, Spilker AC, Gotta M. Control of embryonic spindle positioning and Gα activity by *C. elegans* RIC-8. Curr Biol. 2004; 14:1871–1876. [PubMed: 15498497]

9. Hess HA, Röper JC, Grill SW, Koelle MR. RGS-7 completes a receptor-independent heterotrimeric G protein cycle to asymmetrically regulate mitotic spindle positioning in *C. elegans*. Cell. 2004; 119:209–218. [PubMed: 15479638]

10. Matsuzaki F. *Drosophila* G-protein signalling: Intricate roles for Ric-8? Nat Cell Biol. 2005; 7:1047–1049. [PubMed: 16385732]

11. Tall GG, Gilman AG. Resistance to inhibitors of cholinesterase 8A catalyzes release of Gαi-GTP and nuclear mitotic apparatus protein (NuMA) from NuMA/LGN/Gαi-GDP complexes. Proc Natl Acad Sci U S A. 2005; 102:16584–16589. [PubMed: 16275912]

12. Woodard GE, Huang NN, Cho H, Miki T, Tall GG, Kehrl JH. Ric-8A and Giα recruit LGN, NuMA, and dynein to the cell cortex to help orient the mitotic spindle. Mol Cell Biol. 2010; 30:3519–3530. [PubMed: 20479129]

13. Kerr DS, Von Dannecker LEC, Davalos M, Michaloski JS, Malnic B. Ric-8B interacts with Gαolf and Gγ13 and co-localizes with Gαolf, Gβ1 and Gγ13 in the cilia of olfactory sensory neurons. Mol Cell Neurosci. 2008; 38:341–348. [PubMed: 18462949]

14. Nishimura A, Okamoto M, Sugawara Y, Mizuno N, Yamauchi J, Itoh H. Ric-8A potentiates Gq-mediated signal transduction by acting downstream of G protein-coupled receptor in intact cells. Genes Cells. 2006; 11:487–498. [PubMed: 16629901]

15. Von Dannecker LEC, Mercandante AF, Malnic B. Ric-8B, an olfactory putative GTP exchange factor, amplifies signal transduction through the olfactory-specific G-protein Gαolf. J Neurosci. 2005; 25:3793–3800. [PubMed: 15829631]

16. Von Dannecker LEC, Mercadante AF, Malnic B. Ric-8B promotes functional expression of odorant receptors. Proc Natl Acad Sci U S A. 2006; 103:9310–9314. [PubMed: 16754875]

17. Zhuang H, Matsunami H. Synergism of accessory factors in functional expression of mammalian odorant receptors. J Biol Chem. 2007; 282:15284–15293. [PubMed: 17387175]

18. David NB, Martin CA, Segalen M, Rosenfeld F, Schweisguth F, Bellaïche Y. *Drosophila* Ric-8 regulates Gαi cortical localization to promote Gαi-dependent planar orientation of the mitotic spindle during asymmetric cell division. Nat Cell Biol. 2005; 7:1083–1090. [PubMed: 16228010]

19. Hampoelz B, Hoeller O, Bowman SK, Dunican D, Knoblich JA. *Drosophila* Ric-8 is essential for plasma-membrane localization of heterotrimeric G proteins. Nat Cell Biol. 2005; 7:1099–1105. [PubMed: 16228011]

20. Wang H, Ng KH, Qian H, Siderovski DP, Chia W, Yu F. Ric-8 controls *Drosophila* neural progenitor asymmetric division by regulating heterotrimeric G proteins. Nat Cell Biol. 2005; 7:1091–1098. [PubMed: 16228012]

21. Afshar K, Willard FS, Colombo K, Siderovski DP, Gönczy P. Cortical localization of the Gα protein GPA-16 requires RIC-8 function during *C. elegans* asymmetric cell division. Development. 2005; 132:4449–4459. [PubMed: 16162648]

22. Nagai Y, Nishimura A, Tago K, Mizuno N, Itoh H. Ric-8B stabilizes the α subunit of stimulatory G protein by inhibiting its ubiquitination. J Biol Chem. 2010; 285:11114–11120. [PubMed: 20133939]

23. Chan P, Gabay M, Wright FA, Kan W, Oner SS, Lanier SM, Smrcka AV, Blumer JB, Tall GG. Purification of heterotrimeric G protein α subunits by GST-Ric-8 association: Primary characterization of purified Gαolf. J Biol Chem. 2011; 286:2625–2635. [PubMed: 21115479]

24. Farr GW, Scharl EC, Schumacher RJ, Sondek S, Horwich AL. Chaperonin-mediated folding in the eukaryotic cytosol proceeds through rounds of release of native and nonnative forms. Cell. 1997; 89:927–937. [PubMed: 9200611]

25. Wells CA, Dingus J, Hildebrandt JD. Role of the chaperonin CCT/TRiC complex in G protein βγ-dimer assembly. J Biol Chem. 2006; 281:20221–20232. [PubMed: 16702223]

26. Dupré DJ, Robitaille M, Richer M, Ethier N, Mamarbachi AM, Hébert TE. Dopamine receptor-interacting protein 78 acts as a molecular chaperone for Gγ subunits before assembly with Gβ. J Biol Chem. 2007; 282:13703–13715. [PubMed: 17363375]

27. Lukov GL, Baker CM, Ludtke PJ, Hu T, Carter MD, Hackett RA, Thulin CD, Willardson BM. Mechanism of assembly of G protein βγ subunits by protein kinase CK2-phosphorylated phosducin-like protein and the cytosolic chaperonin complex. J Biol Chem. 2006; 281:22261–22274. [PubMed: 16717095]

28. Lukov GL, Hu T, McLaughlin JN, Hamm HE, Willardson BM. Phosducin-like protein acts as a molecular chaperone for G protein βγ dimer assembly. EMBO J. 2005; 24:1965–1975. [PubMed: 15889144]

29. Rehm A, Ploegh HL. Assembly and intracellular targeting of the βγ subunits of heterotrimeric G proteins. J Cell Biol. 1997; 137:305–317. [PubMed: 9128244]

30. Dupré DJ, Robitaille M, Rebois RV, Hébert TE. The role of Gβγ subunits in the organization, assembly, and function of GPCR signaling complexes. Annu Rev Pharmacol Toxicol. 2009; 49:31–56. [PubMed: 18834311]

31. Willardson BM, Howlett AC. Function of phosducin-like proteins in G protein signaling and chaperone-assisted protein folding. Cell Signal. 2007; 19:2417–2427. [PubMed: 17658730]

32. Linder ME, Middleton P, Hepler JR, Taussig R, Gilman AG, Mumby SM. Lipid modifications of G proteins: α subunits are palmitoylated. Proc Natl Acad Sci U S A. 1993; 90:3675–3679. [PubMed: 8475115]

33. Marrari Y, Crouthamel M, Irannejad R, Wedegaertner PB. Assembly and trafficking of heterotrimeric G proteins. Biochemistry. 2007; 46:7665–7677. [PubMed: 17559193]

34. Mumby SM, Heukeroth RO, Gordon JI, Gilman AG. G-protein α-subunit expression, myristoylation, and membrane association in COS cells. Proc Natl Acad Sci U S A. 1990; 87:728–732. [PubMed: 2153964]

35. Jones TL, Simonds WF, Merendino JJ Jr, Brann MR, Spiegel AM. Myristoylation of an inhibitory GTP-binding protein α subunit is essential for its membrane attachment. Proc Natl Acad Sci U S A. 1990; 87:568–572. [PubMed: 2105488]

36. Preininger AM, Parello J, Meier SM, Liao G, Hamm HE. Receptor-mediated changes at the myristoylated amino terminus of Gα$_{il}$ proteins. Biochemistry. 2008; 47:10281–10293. [PubMed: 18771287]

37. Hughes TE, Zhang H, Logothetis DE, Berlot CH. Visualization of a functional Gα$_q$-green fluorescent protein fusion in living cells. Association with the plasma membrane is disrupted by mutational activation and by elimination of palmitoylation sites, but not by activation mediated by receptors or AIF4−. J Biol Chem. 2001; 276:4227–4235. [PubMed: 11076942]

38. Ransnas LA, Svoboda P, Jasper JR, Insel PA. Stimulation of β-adrenergic receptors of S49 lymphoma cells redistributes the α subunit of the stimulatory G protein between cytosol and membranes. Proc Natl Acad Sci U S A. 1989; 86:7900–7903. [PubMed: 2554294]

39. Svoboda P, Novotny J. Hormone-induced subcellular redistribution of trimeric G proteins. Cell Mol Life Sci. 2002; 59:501–512. [PubMed: 11964127]

40. Wedegaertner PB, Bourne HR, von Zastrow M. Activation-induced subcellular redistribution of Gs$_α$. Mol Biol Cell. 1996; 7:1225–1233. [PubMed: 8856666]

41. Tsutsumi R, Fukata Y, Noritake J, Iwanaga T, Perez F, Fukata M. Identification of G protein α subunit-palmitoylating enzyme. Mol Cell Biol. 2009; 29:435–447. [PubMed: 19001095]

42. Chisari M, Saini DK, Kalyanaraman V, Gautam N. Shuttling of G protein subunits between the plasma membrane and intracellular membranes. J Biol Chem. 2007; 282:24092–24098. [PubMed: 17576765]

43. Tõnissoo T, Lulla S, Meier R, Saare M, Ruisu K, Pooga M, Karis A. Nucleotide exchange factor RIC-8 is indispensable in mammalian early development. Dev Dyn. 2010; 239:3404–3415. [PubMed: 21069829]

44. Valenzuela DM, Murphy AJ, Frendewey D, Gale NW, Economides AN, Auerbach W, Poueymirou WT, Adams NC, Rojas J, Yasenchak J, Chernomorsky R, Boucher M, Elsasser AL, Esau L, Zheng J, Griffiths JA, Wang X, Su H, Xue Y, Dominguez MG, Noguera I, Torres R, Macdonald LE, Stewart AF, DeChiara TM, Yancopoulos GD. High-throughput engineering of the mouse genome

coupled with high-resolution expression analysis. Nat Biotechnol. 2003; 21:652–659. [PubMed: 12730667]

45. Nichols J, Zevnik B, Anastassiadis K, Niwa H, Klewe-Nebenius D, Chambers I, Schöler H, Smith A. Formation of pluripotent stem cells in the mammalian embryo depends on the POU transcription factor Oct4. Cell. 1998; 95:379–391. [PubMed: 9814708]

46. Siderovski DP, Willard FS. The GAPs, GEFs, and GDIs of heterotrimeric G-protein α subunits. Int J Biol Sci. 2005; 1:51–66. [PubMed: 15951850]

47. Hynes TR, Tang L, Mervine SM, Sabo JL, Yost EA, Devreotes PN, Berlot CH. Visualization of G protein βγ dimers using bimolecular fluorescence complementation demonstrates roles for both β and γ in subcellular targeting. J Biol Chem. 2004; 279:30279–30286. [PubMed: 15136579]

48. Mumby SM, Kahn RA, Manning DR, Gilman AG. Antisera of designed specificity for subunits of guanine nucleotide-binding regulatory proteins. Proc Natl Acad Sci U S A. 1986; 83:265–269. [PubMed: 3079909]

49. Linder ME, Ewald DA, Miller RJ, Gilman AG. Purification and characterization of $G_{o\alpha}$ and three types of $G_{i\alpha}$ after expression in *Escherichia coli*. J Biol Chem. 1990; 265:8243–8251. [PubMed: 2159473]

50. Tang WJ, Gilman AG. Adenylyl cyclases. Cell. 1992; 70:869–872. [PubMed: 1525824]

51. Hart MJ, Jiang X, Kozasa T, Roscoe W, Singer WD, Gilman AG, Sternweis PC, Bollag G. Direct stimulation of the guanine nucleotide exchange activity of p115 RhoGEF by $G\alpha_{13}$. Science. 1998; 280:2112–2114. [PubMed: 9641916]

52. Krumins AM, Gilman AG. Targeted knockdown of G protein subunits selectively prevents receptor-mediated modulation of effectors and reveals complex changes in non-targeted signaling proteins. J Biol Chem. 2006; 281:10250–10262. [PubMed: 16446365]

53. Klattenhoff C, Montecino M, Soto X, Guzmán L, Romo X, de los Angeles García M, Mellstrom B, Naranjo JR, Hinrichs MV, Olate J. Human brain synembryn interacts with Gsα and Gqα and is translocated to the plasma membrane in response to isoproterenol and carbachol. J Cell Physiol. 2003; 195:151–157. [PubMed: 12652642]

54. Malik S, Ghosh M, Bonacci TM, Tall GG, Smrcka AV. Ric-8 enhances G protein βγ-dependent signaling in response to βγ-binding peptides in intact cells. Mol Pharmacol. 2005; 68:129–136. [PubMed: 15802611]

55. Mumby SM, Gilman AG. Synthetic peptide antisera with determined specificity for G protein α or β subunits. Methods Enzymol. 1991; 195:215–233. [PubMed: 1903488]

56. Gutowski S, Smrcka A, Nowak L, Wu DG, Simon M, Sternweis PC. Antibodies to the α_q subfamily of guanine nucleotide-binding regulatory protein α subunits attenuate activation of phosphatidylinositol 4,5-bisphosphate hydrolysis by hormones. J Biol Chem. 1991; 266:20519–20524. [PubMed: 1657928]

57. Pang IH, Sternweis PC. Purification of unique α subunits of GTP-binding regulatory proteins (G proteins) by affinity chromatography with immobilized βγ subunits. J Biol Chem. 1990; 265:18707–18712. [PubMed: 2120237]

58. Singer WD, Miller RT, Sternweis PC. Purification and characterization of the α subunit of G_{13}. J Biol Chem. 1994; 269:19796–19802. [PubMed: 8051060]

59. Hein P, Rochais F, Hoffmann C, Dorsch S, Nikolaev VO, Engelhardt S, Berlot CH, Lohse MJ, Bünemann M. G_S activation is time-limiting in initiating receptor-mediated signaling. J Biol Chem. 2006; 281:33345–33351. [PubMed: 16963443]

60. Liu Q, Li MZ, Leibham D, Cortez D, Elledge SJ. The univector plasmid-fusion system, a method for rapid construction of recombinant DNA without restriction enzymes. Curr Biol. 1998; 8:1300–1309. [PubMed: 9843682]

61. Narayanan K, Williamson R, Zhang Y, Stewart AF, Ioannou PA. Efficient and precise engineering of a 200 kb β-globin human/bacterial artificial chromosome in *E. coli* DH10B using an inducible homologous recombination system. Gene Ther. 1999; 6:442–447. [PubMed: 10435094]

62. Yang XW, Model P, Heintz N. Homologous recombination based modification in *Escherichia coli* and germline transmission in transgenic mice of a bacterial artificial chromosome. Nat Biotechnol. 1997; 15:859–865. [PubMed: 9306400]

63. Zhang Y, Buchholz F, Muyrers JPP, Stewart AF. A new logic for DNA engineering using recombination in *Escherichia coli*. Nat Genet. 1998; 20:123–128. [PubMed: 9771703]

64. Nagy, A.; Gertsenstein, M.; Vintersen, K.; Behringer, R. Manipulating the Mouse Embryo: A Laboratory Manual. Cold Spring Harbor Laboratory Press; Cold Spring Harbor, NY: 2003.

65. Schaffner W, Weissmann C. A rapid, sensitive, and specific method for the determination of protein in dilute solution. Anal Biochem. 1973; 56:502–514. [PubMed: 4128882]

66. Livak KJ, Schmittgen TD. Analysis of relative gene expression data using real-time quantitative PCR and the $2^{-\Delta\Delta C_T}$ method. Methods. 2001; 25:402–408. [PubMed: 11846609]
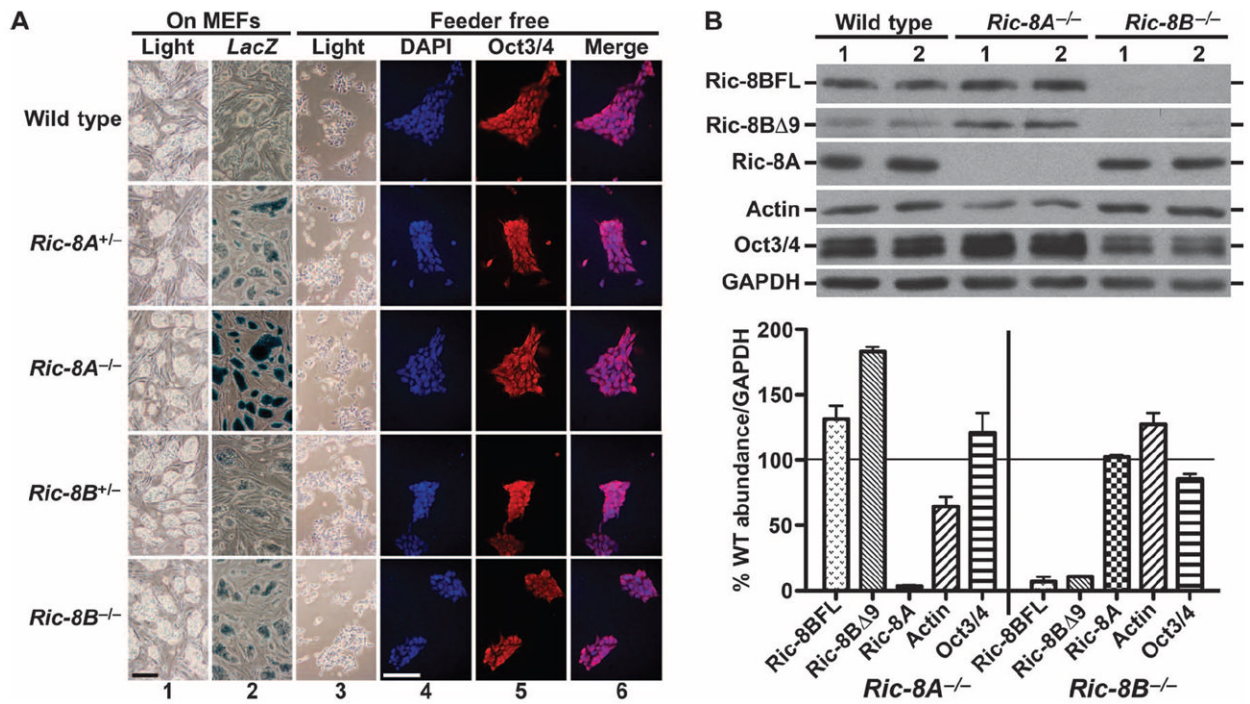
Fig. 1.
Mouse ES cell lines derived from blastocysts deficient in *Ric-8A* or *Ric-8B* are viable. (**A**) Wild-type (C57BL/6J), *Ric-8A^{+/−}^*, *Ric-8A^{−/−}^*, *Ric-8B^{+/−}^*, and *Ric-8B^{−/−}^* mES cell lines were derived from blastocysts and cultured on mitotically inactivated wild-type MEFs (columns 1 and 2) and adapted to grow in feeder-free culture (columns 3 to 6). β-Galactosidase activity from *LacZ* transgenes under control of the endogenous *Ric-8A* or *Ric-8B* promoters was measured in each cell line (column 2). mES colonies were costained with DAPI (column 4) and with antibody against Oct3/4 (column 5) to show homogeneous Oct3/4 abundance (Merge, column 6). Scale bar, 200 μm. (**B**) Quantitative Western blotting analysis of the amounts of Ric-8A, Ric-8B, actin, Oct3/4, and GAPDH was performed with whole-cell lysates prepared from two independently derived wild-type (WT), *Ric-8A^{−/−}^*, and *Ric-8B^{−/−}^* mES cell lines. The amounts of the indicated proteins relative to that of GAPDH were quantified by pixel densitometry analysis with Adobe Photoshop 4.0 (Adobe Systems Inc.). Error bars represent the means ± SEM of three experiments with averaged results from two independent cell lines of each genotype.
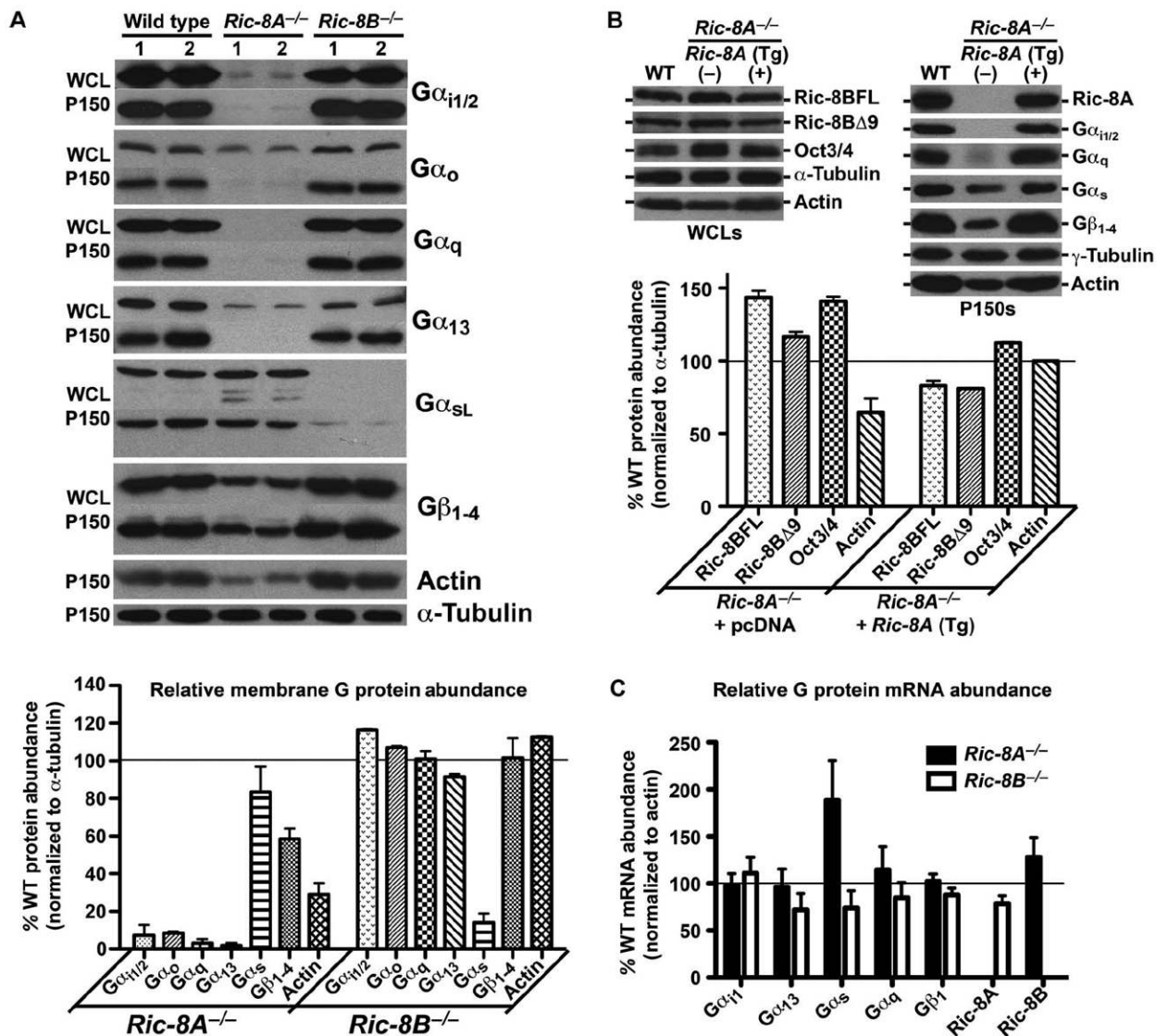
Fig. 2.
Steady-state amounts of heterotrimeric G proteins are selectively abrogated in *Ric-8A–* or *Ric-8B*–deleted mES cells. (**A**) Whole-cell lysates (WCL) or crude membrane fractions (from 150,000*g* centrifugation, P150) prepared from two independently derived wild-type, *Ric-8A*$^{-/-}$, and *Ric-8B*$^{-/-}$ mES cell lines were subjected to quantitative Western blotting for actin, α-tubulin, and the G protein subunits Gα$_{i1/2}$, Gα$_o$, Gα$_q$, Gα$_{13}$, Gα$_s$, and total Gβ$_1$. The amounts of the indicated proteins in membrane fractions compared to that of α-tubulin were quantified by pixel densitometry, as described earlier. Error bars represent the means ± SEM obtained from duplicate cell lines of each genotype. (**B**) Stable expression of the *Ric-8A* cDNA as a trans-gene (Tg) in a *Ric-8A*$^{-/-}$ cell line restored G protein and actin protein amounts as determined by quantitative Western blotting. Error bars represent the means ± SEM. (**C**) Relative amounts of Gα$_{i1}$, Gα$_{13}$, Gα$_s$, Gα$_q$, Gβ$_1$, Ric-8A, and Ric-8B mRNAs in *Ric-8A*$^{-/-}$ and *Ric-8B*$^{-/-}$ cell lines were measured by quantitative real-time PCR. Error bars represent the means ± SEM obtained from duplicate, independently derived cell lines of each genotype.
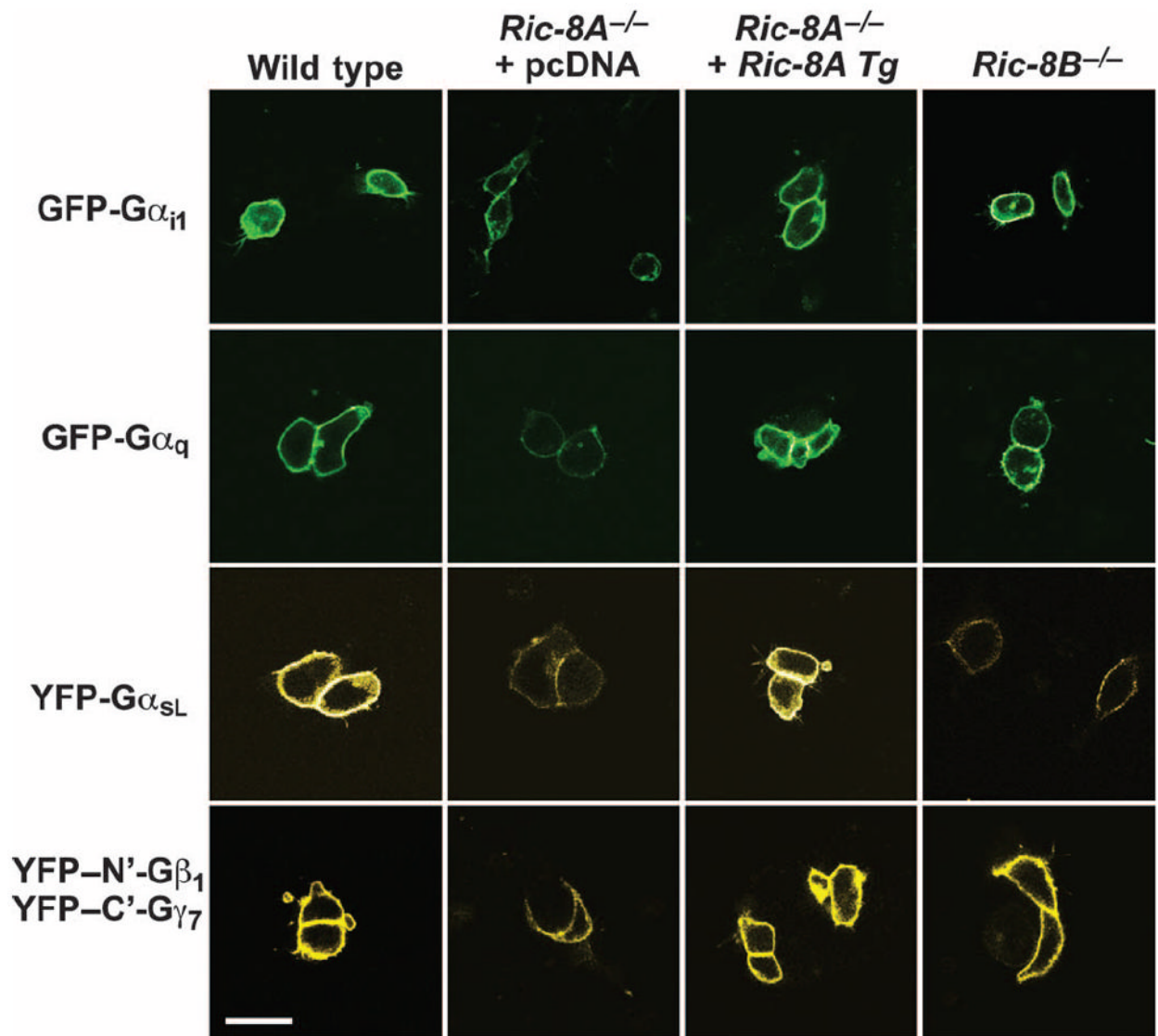
Fig. 3.
G proteins are localized less efficiently at the plasma membrane in *Ric-8A–* or *Ric-8B–* deleted mES cells than in wild-type cells. Wild-type mES cells, *Ric-8A*$^{-/-}$ mES cells stably expressing pcDNA or *Ric-8A* cDNA transgene (Tg), and *Ric-8B*$^{-/-}$ mES cells were transiently transfected with plasmids encoding GFP-Gα_{i1}, GFP-Gα_q, and YFP-Gα_{sL} or the split YFP constructs, YFP–N′-Gβ_1 and YFP–C′-Gγ_7. Cells were visualized by confocal fluorescence microscopy. The signal gain in these images was uniformly enhanced to observe the weak plasma membrane–localized fluorescence of G proteins in the respective *Ric-8*$^{-/-}$ cells. The enhancement resulted in some saturated cell images, such that the apparent differences in G protein plasma membrane signal intensity are not linear. Scale bar, 20 µm.
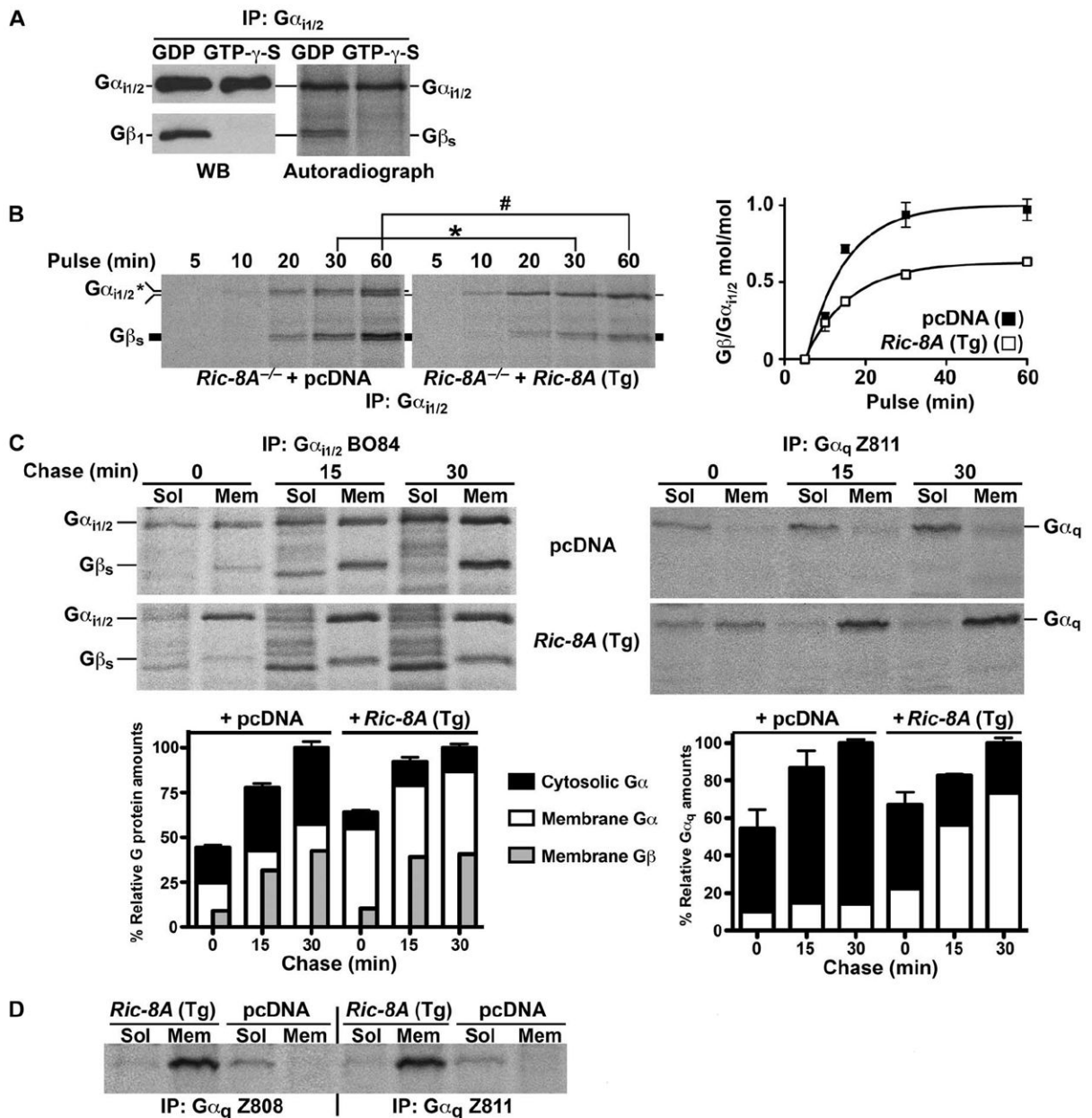
Fig. 4.
Nascent $G\alpha_{i1/2}$ and $G\alpha_q$ are defective in their initial association with the membrane in *Ric-8A*–deleted mES cells. (**A**) Nucleotide-dependent coimmunoprecipitation of endogenous $G\alpha_{i1/2}$ and $G\beta$ subunits. WCLs from wild-type mES cells that were metabolically labeled with [^{35}S]methionine and [^{35}S]cysteine for 1 hour and were supplemented with GDP or Mg^{+2}–GTP-γ-S were subjected to immunoprecipitation (IP) with antiserum against $G\alpha_{i1/2}$. The immunoprecipitated samples were resolved by SDS-PAGE and subjected to autoradiography or were analyzed by Western blotting (WB) for $G\alpha_{i1/2}$ and $G\beta_1$. (**B**) Nascent $G\alpha_{i1/2}$ synthesis and association with nascent $G\beta$ subunits over a 1-hour time course of metabolic pulse labeling. *Ric-8A*$^{-/-}$ mES cells expressing pcDNA or *Ric-8A* (Tg) were metabolically labeled for the indicated times. WCLs were prepared and subjected to quantitative immunoprecipitation with antiserum against $G\alpha_{i1/2}$. Immunoprecipitated $G\alpha_{i1/2}$

and associated Gβ subunits were resolved by SDS-PAGE and visualized by autoradiography. Molar ratios of the amount of Gβ to that of $G\alpha_{i1/2}$ were quantified by pixel densitometry, as described earlier, after factoring in a 22:18 ratio of methionines and cysteines within the two processed proteins. Error bars represent the means ± SEM of three independent experiments. *P < 0.0085; #P < 0.0091. (**C**) Subcellular fractionation of newly synthesized $G\alpha_q$ and $G\alpha_{i1/2}$ with associated nascent Gβ subunits was measured after metabolic pulse (10 min) and chase (to 30 min) labeling of *Ric-8A*$^{-/-}$ cells expressing sham cDNA or *Ric-8A* cDNA. Labeled proteins were immunoprecipitated from cytosolic (Sol) and crude membrane (Mem) fractions and subjected to quantitative autoradiography. Error bars on the accompanying histographs represent the means ± SEM of three independent experiments. (**D**) Metabolic 2-hour pulse-labeling and subcellular fractionation analysis of $G\alpha_q$ in cytosolic (Sol) and crude membrane (Mem) fractions was measured by immunoprecipitation with antisera against $G\alpha_q$ (Z808 and Z811). The panel shown is representative of three independent experiments.
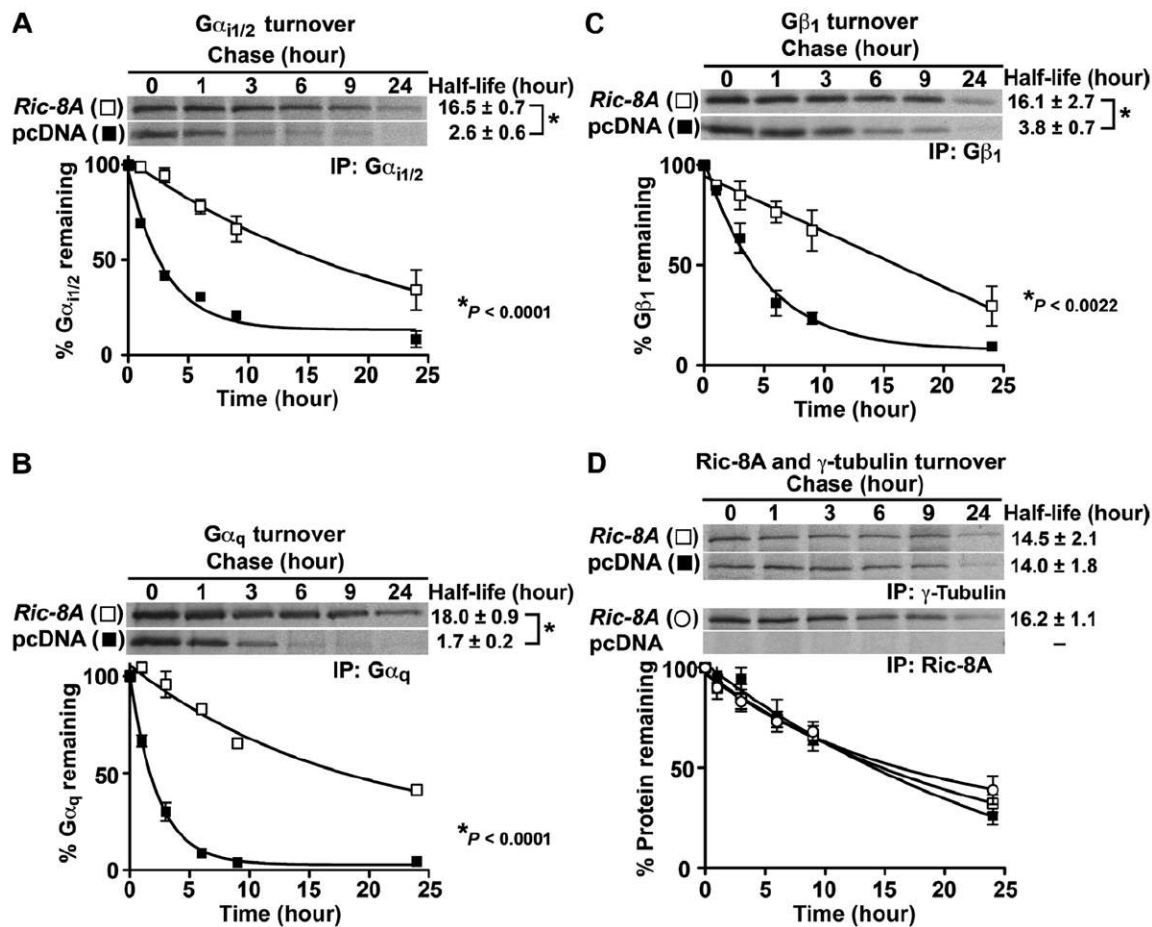
Fig. 5.
Newly synthesized Gα subunits and Gβ₁ are degraded rapidly in *Ric-8A⁻/⁻* mES cells. *Ric-8A⁻/⁻* cells stably expressing *Ric-8A* (Tg) or pcDNA were pulse-labeled with [³⁵S]methionine and [³⁵S]cysteine for 1 hour and chased in the presence of unlabeled amino acids for 0 to 24 hours. (**A** to **D**) Endogenous $G\alpha_{i1/2}$ (A), $G\alpha_q$ (B), $G\beta_1$ (C), and γ-tubulin (D) and stably expressed Ric-8A were immunoprecipitated at each time point, resolved by SDS-PAGE, and visualized by autoradiography. The percentages of proteins that remained with time were quantified by pixel densitometry analysis as described earlier. The data were fit to monoexponential turnover functions to calculate half-lives with GraphPad Prism 5.0 software. Error bars represent the means ± SEM of three independent experiments.
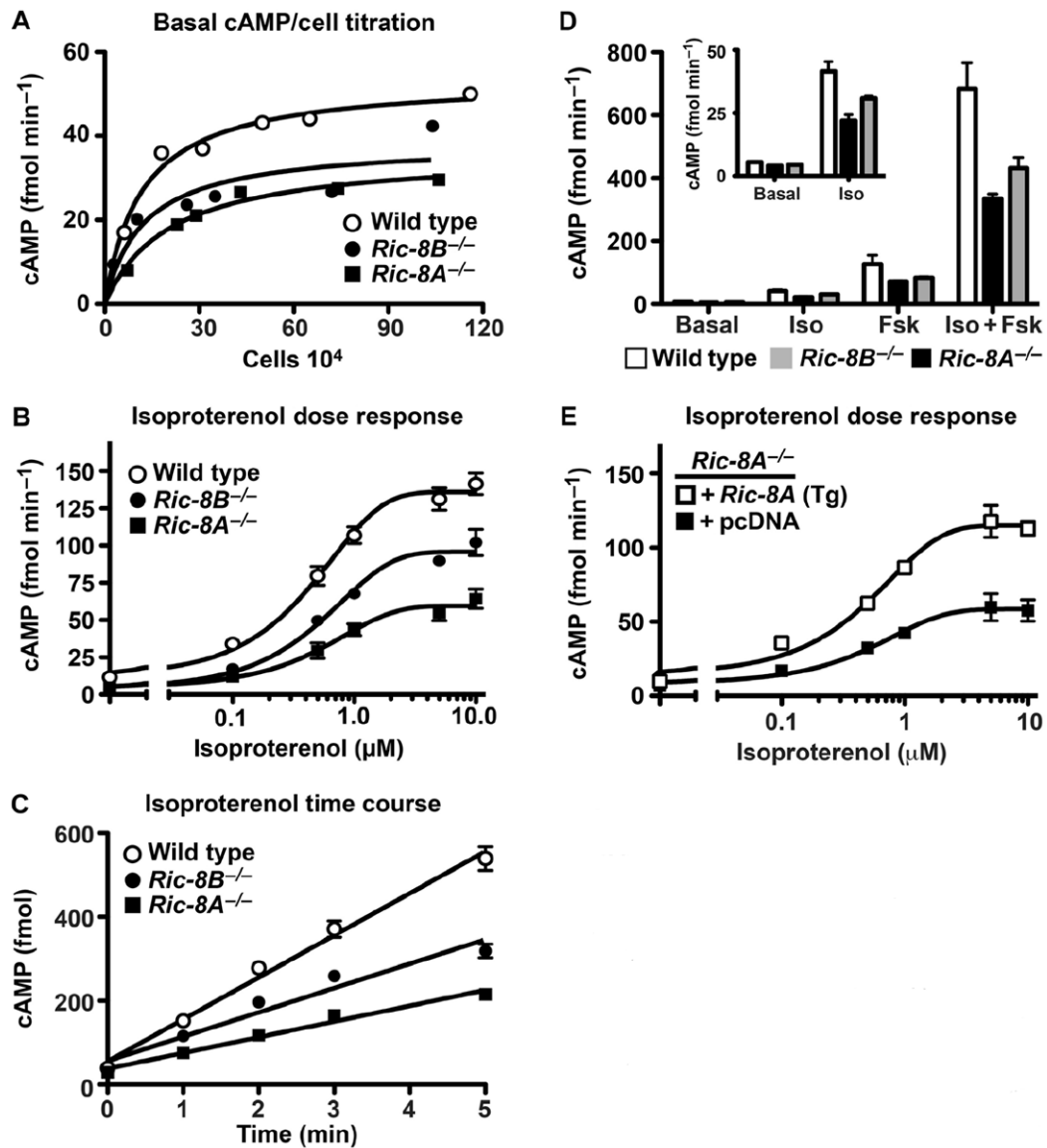
Fig. 6.
Basal and β-AR–stimulated AC activity is attenuated in *Ric-8A*– and *Ric-8B*–deleted mES cells. (**A**) Wild-type, *Ric-8A*$^{-/-}$, and *Ric-8B*$^{-/-}$ (1×10^4 to 75×10^4) mES cell lines were seeded in duplicate 96-well plates 24 hours before basal cAMP measurements were made. Cell counts were determined from one parallel plate at the time of basal cAMP measurement. Results are the average of two independent experiments from duplicate cell lines of each genotype. (**B**) Accumulated cAMP was measured after treatment of cells with isoproterenol (0 to 10 μM) for 2 min at 22°C. Error bars represent the means ± SEM for three independent experiments with duplicate cell lines of each genotype. (**C**) Accumulated cAMP was measured after cell treatment with a saturating concentration of isoproterenol (10 μM) for the indicated times at 22°C. Error bars represent the means ± SEM for three independent experiments with duplicate cell lines of each genotype. (**D**) Basal and accumulated cAMP amounts were measured after cell treatment with vehicle (basal), isoproterenol (100 nM, EC$_{20}$), forskolin (50 μM, EC$_{20}$), or isoproterenol and forskolin (EC$_{20s}$) for 5 min at 22°C. Error bars represent the means ± SEM for three independent

experiments with duplicate cell lines of each genotype. (**E**) Induction of cAMP accumulation by isoproterenol (0 to 10 μM) was measured in *Ric-8A*$^{-/-}$ mES cell lines stably transfected with *Ric-8A* cDNA (Tg) or sham vector. Error bars represent the means ± SEM for three independent experiments.
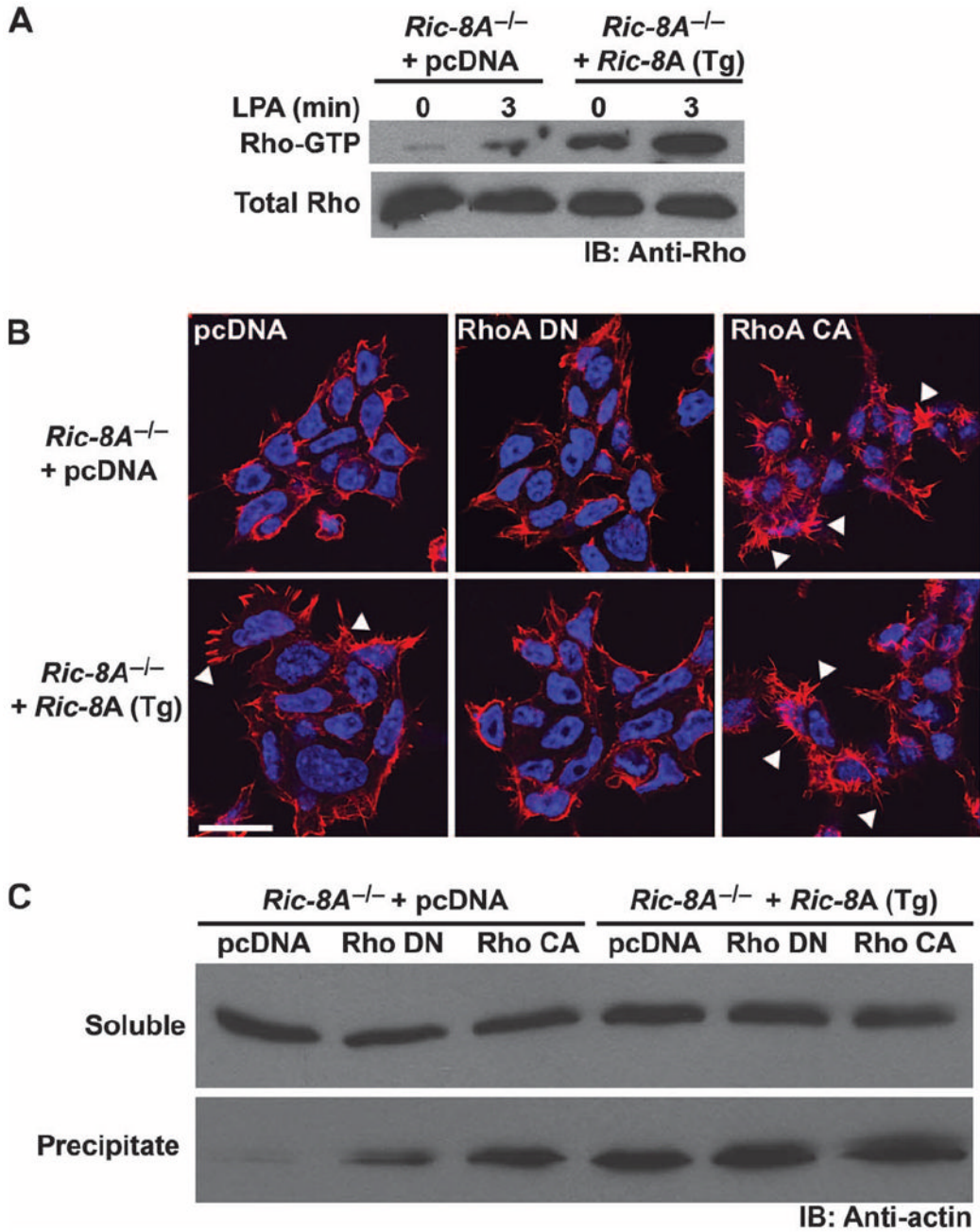
Fig. 7.
Basal and LPA receptor–stimulated Rho signaling is attenuated in *Ric-8A*–deleted mES cells. (**A**) *Ric-8A*$^{-/-}$ cells stably expressing *Ric-8A* or sham cDNA were not stimulated or were stimulated with LPA (10 μM) for 3 min. Rho-GTP was isolated from equivalent amounts of cell lysates in GST-Rhotekin pull-down assays. Relative amounts of total Rho and Rho-GTP were visualized by Western blotting with an antibody against Rho (Anti-Rho). Data are representative of two independent experiments. (**B**) *Ric-8A*$^{-/-}$ cells stably expressing *Ric-8A* (Tg) or sham cDNA were transiently transfected with control plasmid (pcDNA), plasmid encoding dominant-negative (DN) RhoA T19N, or plasmid encoding constitutively active (CA) RhoA G14V. After 48 hours, cells were costained with DAPI and rhodamine-phalloidin to visualize nuclei and F-actin structures, respectively. Arrowheads

denote actin filopodia. Scale bar, 20 μm. Data are representative of three or more independent experiments. (**C**) *Ric-8A*$^{-/-}$ cells stably expressing *Ric-8A* (Tg) or sham cDNA were transiently transfected with pcDNA, *RhoA* (DN), or *RhoA* (CA) and fractionated by centrifugation of postnuclear supernatants at 150,000*g*. Relative amounts of G-actin and F-actin were visualized by Western blotting analysis with antibody against actin (Anti-actin). Data are representative of two independent experiments.
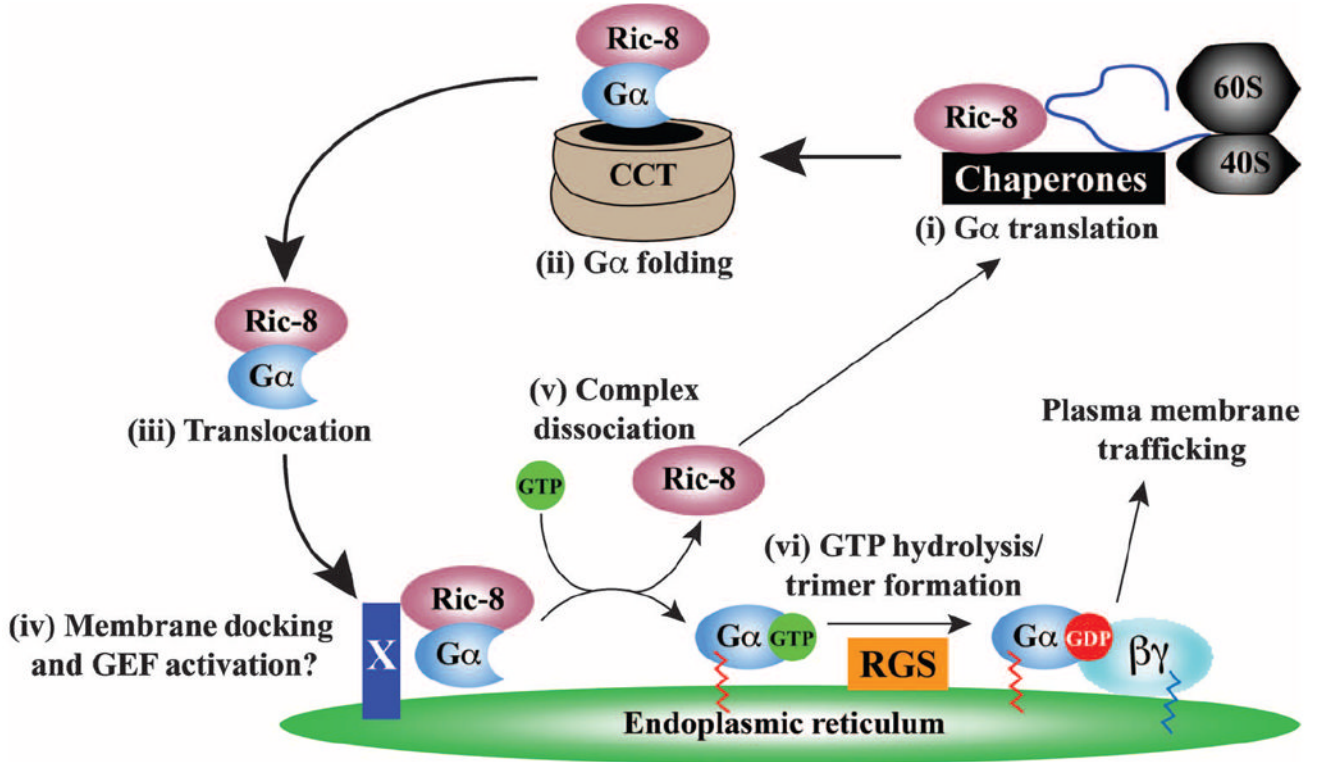
Fig. 8.
Proposed model for the action of Ric-8 during G protein biosynthesis. Gα subunits are translated on free, cytosolic ribosomes. (i) The emerging Gα chain may be bound by Ric-8 and cellular chaperones during initial protein folding, or (ii) it may be folded as part of a ternary complex withCCTand Ric-8. (iii) The nucleotide-free Ric-8–Gα complex then translocates to a putative, ER membrane–specific docking factor (X) that may also serve as the cellular activator (iv) of Ric-8 nucleotide exchange stimulatory activity, enabling production of (v) dissociated Ric-8 and membrane-bound Gα-GTP. (vi) Gα hydrolyzes GTP, perhaps through the aid of organelle-specific RGS GAPs (GTPase-activating proteins). The resultant Gα-GDP binds to Gβγ before the newly formed G protein heterotrimer traffics to the plasma membrane.